An agent-based model clarifies the importance of functional and developmental integration in shaping brain evolution

Shahar Avin[1], Adrian Currie[2#] & Stephen H. Montgomery[3#*]

[1] Centre for the Study of Existential Risk, University of Cambridge
[2] Department of Sociology, Philosophy and Anthropology, University of Exeter
[3] School of Biological Sciences, University of Bristol
[#]contributed equally
*corresponding author: s.montgomery@bristol.ac.uk

Abstract

Comparisons of vertebrate brain structure suggest a conserved pattern of scaling between components, but also many examples of lineages diverging dramatically from these general trends. Two competing hypotheses of brain evolution seek to explain these patterns of variation by invoking either 'external' processes, such as selection in driving phenotypic change, or 'internal' processes, like developmental coupling among brain regions. Efforts to reconcile these views remain deadlocked, in part due to empirical under-determination and the limitations of 'relative significance' debates. We introduce an agent-based model that allows us to simulate brain evolution in a 'bare-bones' system and examine the dependencies between variables that may shape brain evolution. Our simulations formalise verbal arguments and interpretations concerning the evolution of brain structure. We illustrate that 'concerted' patterns of brain evolution cannot alone be taken as evidence for developmental coupling, or constraint, despite these terms often being treated as synonymous. Both developmentally coupled and uncoupled brain architectures can represent adaptive strategies, depending on the distribution of selection across the brain, life history, and the relative costs of neural tissue. Our model also illustrates how the importance of mosaic and concerted patterns of evolution may fluctuate through time in a variable environment, which we argue implies that developmental coupling is unlikely to be a significant evolutionary constraint.

Key words

Brain structure, brain size, constraint, concerted evolution, mosaic evolution, neuro-evo-devo.

Introduction

How are macro-evolutionary patterns in vertebrate brain structure best characterised, and what processes drive those patterns? Answering these questions requires understanding how developmental mechanisms or architectural constraints, as well as selection acting on neural traits, together shape and support behavioural and cognitive evolution. Debates over these conflicting pressures on variation have dominated vertebrate evolutionary neurobiology for decades, with no unified theoretical framework in sight.

At the heart of this debate are two views of brain evolution which, at their most polarized, make diametrically opposing predictions. Under one hypothesis, brain components are developmentally coupled such that the size of each component is largely determined by common developmental mechanisms, such as the timing and duration of neurogenesis (1). This would lead the entire brain to evolve in a 'concerted' manner, with the size of all components being closely predicted by overall brain size (1–3). Initially, this coupling was viewed as an evolutionary constraint (2) and, although proponents of this hypothesis now argue that developmental coupling is a mechanism that evolved in response to selection favouring conservative scaling (1,4), the view that concertedness indicates developmental constraint remains widespread in the literature (e.g. 5-11). A contrasting hypothesis instead argues that variation in brain components is developmentally independent of both other brain structures, and of total brain size, allowing them to respond to targeted selection pressures in a 'mosaic' way (12–16). Mosaic evolution can lead to adaptive, non-allometric changes in brain structure, with stabilizing selection otherwise maintaining scaling relationships between co-evolving, functionally interdependent brain components (14,17). In essence, the mosaic model favours 'external' explanations that emphasize the role of selection in driving both independent phenotypic evolution *and* co-variation of brain structures, while concerted theorists favor 'internal' mechanisms which emphasise the role of developmental coupling as a route to maintaining scaling relationships (18).

Perhaps confusingly both hypotheses have at times been supported by analyses of the same volumetric data (2,14,19). Proponents of the 'concerted' view of brain evolution point to the consistent allometric scaling between brain components and total brain size as evidence of strong developmental integration across brain structures (1,2). Proponents of the 'mosaic' model instead point towards co-evolution between brain components that is independent of total brain size, and evidence for 'grade shifts' that indicate deviations in scaling between taxonomic groups, as

evidence that brain components are caught between distinct selection pressures, and the constraint of functional-interdependence (14). Distinctions between these hypotheses have become more nuanced, with the concerted hypothesis incorporating periodic restructuring of the brain (4,20). However, universally satisfactory tests of these hypotheses have proven elusive.

There are two key reasons for this deadlock. First, proponents of concerted and mosaic models are engaged in a 'relative significance debate' (21). Both sides agree that brain evolution exhibits features associated with both concerted and mosaic evolution, but disagree on which pattern dominates across evolutionary time, and why (for example, see ref. 1, p. 299). Relative significance makes hypothesis testing difficult. Neither hypothesis is subject to critical tests, as both accommodate - and even expect - different degrees of departure from the 'norm'. Competing views of brain evolution therefore run the risk of being too indeterminate for definitive testing.

Second, tests of these hypotheses are underdetermined by available evidence. Empirical support for concerted or mosaic evolution is most often drawn from comparative analyses of volumetric brain data. These data reflect the outcome of the interaction between competing adaptive and constraining factors, and do not, in themselves, provide evidence of the developmental mechanisms involved (22,23). This is a critical point, as 'concertedness' has frequently become a byword for developmental constraint (e.g. 5-11), biasing the interpretation and presentation of many studies. This is problematic because the mosaic brain hypothesis also predicts co-variation between interdependent brain regions. If one views the brain as a network of interdependent networks, these *functional* constraints could produce consistent scaling relationships across brain components— *i.e.* concerted evolution— without invoking developmental coupling (17). Merely recognising a concerted pattern is therefore insufficient evidence to assess competing mechanisms, or support the predominance of either hypothesis.

If patterns of phenotypic variation alone are unsuitable for identifying the mechanisms underpinning allometric scaling, what evidence could? As noted by previous authors, "it is not the *phenotypic* correlation that matters, so much as the *genetic* correlation" (24). Several recent quantitative genetics studies have found evidence of substantial genetic independence between brain components (5,8,25), a central prediction of the mosaic brain hypothesis (reviewed in 17). However, these studies typically concern standing genetic variation within populations. The developmental coupling hypothesis can accommodate this evidence if much of this genetic variation will be deleterious, and therefore does not reflect the genetic architecture favoured by

selection over evolutionary timescales. Hence, neither phenotypic data nor currently available genetic data, are sufficient to unite views on the relative importance of developmental and functional coupling, constraint, and adaptive lability in the evolution of brain structure.

When faced with relative significance and empirical underdetermination, simple mathematical models can help realise basic causal dynamics in a 'bare-bones' system, and are a way of examining the dependencies between variables that are thought to be important. Such models can inform empirical studies by making explicit hitherto hidden assumptions, and revealing surprising emergent dynamics (26). This approach has recently been applied to debates over the socio-ecological selection pressures shaping brain size (27–30), providing a new approach to the field of evolutionary neurobiology. Here, we introduce an agent-based model of brain structure that allows us to explore the interactions between fitness and constraints derived from selection, development and function. In particular our model allows us to formalise several verbal arguments over the role of developmental coupling in brain evolution:

1. Do functional dependencies produce concerted patterns of evolution as well as developmental coupling (c.f. 22,23)?
2. Do costs of neural tissue select against concertedness when selection acts on a specific brain component (c.f. 31)?
3. Is developmental integration evolutionarily labile (c.f. 32), and do functional dependencies select for developmental coupling (c.f. 22,32)?
4. Does developmental coupling allow brains to evolve adaptively, quicker (1)?

Our model allows us to explore these previously verbal arguments and interpretations of volumetric data. We demonstrate that this 'bare-bones' model helps clarify current debates surrounding the evolution of brain structure by capturing the basic evolutionary dynamics at play, and hope that it shifts these debates in a productive theoretical and empirical direction.

Methods

To explore the interplay between developmental and functional coupling on the evolution of brain structure, we devised a model that simulates the evolution of a population of individuals in an environment, where fitness is determined by the size and costs of brain components.

i) Model components

The model is characterized by three components: the population of individuals, the environment, and an evolutionary algorithm. We provide a simplified description of the model in Figure S1.

Each individual is characterized by a number (*N*) of *brain components*, each component having a specific *size* ($S_{i,j}$), where *i* denotes the individual and *j* denotes the *j*-th of *N* components. For example, among individuals with three brain components (*N*=3), the brain of 'Individual A' could have a first component of size $S_{A,1}$=5, a second component of size $S_{A,2}$=7, and a third component of size $S_{A,3}$=2, which we denote as S_A=(5, 7, 2). A second individual, 'Individual B', might have component brain sizes of 3, 3 and 1 respectively, denoted S_B=(3, 3, 1). In this case the total size of Individual A's brain would be 14, while the size of Individual B's brain would be 7. Our model assumes that all brain components have the same fitness cost per unit size (see below), so it is total brain size that determines the evolutionary cost of an individual's brain, while the size of individual components contribute differently to fitness benefits. Whether evolution is mosaic or concerted depends upon the factors influencing changes in brain component sizes over time. The sizes of brain components are allowed to vary, through mutation, and this variation is influenced by *developmental coupling* (*D*), which takes values between 0.0 (no developmental coupling, i.e. a fully 'mosaic' brain) and 1.0 (complete developmental coupling, i.e. a brain structure fully determined by total brain size). *D* is analogous to the strength of genetic correlations between components. For example, a *D* of 0.5, would indicate that 50% of the variation in each component is determined by variation in total brain size, and 50% of the variation in each brain component is independent of variation in both total brain size and other components. When a mutation event occurs, the program generates *N*+1 random mutation factors (m_i), for example between 0.5 and 1.5 for a 50% mutation step size, where there is one factor is for the whole brain (m_0) and one for each component (m_1 to m_N). Each brain component is then scaled by these mutation factors, with the variation in mutations affecting particular brain components being flattened depending on *D's* value. For example, when *D* is 0, m_0 for total brain size mutation will be multiplied by 0 but other mutation factors will vary independently according to a scaling factor (1 – *D,* i.e. unscaled when *D* is 0), whereas when *D* is 1 all mutation factors for individual brain components will be multiplied by 0 and only the mutation factor for total brain size will persist. Models with intermediate values of *D* fall between these extremes. This is determined according to the following formula.

$$(1)\ S_{i,j(new)} = \left[(D * m_0) + \left((1 - D) * m_i\right)\right] * S_{i,j(old)}; j \in \{1, \dots, N\}$$

The *Environment* is characterized by three factors. First, a set of *benefits* (B_j), one for each of the *N* brain components, which represents the fitness contribution of each size unit an individual gains from that particular brain component, at a particular size. For example, in an environment with benefits *B*=(1, 2, 3), 'Individual A' from above will have total fitness contributions from brain component sizes of 5*1 + 7*2 + 2*3 = 25, while 'Individual B' will have total fitness benefits of 3*1 + 3*2 + 1*3 = 12. Second, the environment imposes a fitness *cost* (*C*) per size unit of brain, which is uniform for all brain components based on the assumption that there is a linear 'per neuron' energetic cost (33), and that units of 'size' in the model is analogous to neuron number. Total fitness for an individual *i* with brain component sizes $S_{i,j}$ in an environment defined by benefits B_j and cost *C* is thus given by $\sum_j (S_{i,j} * B_j) - (C * \sum_j S_{i,j})$. For example, if the environment described above had a cost *C*=1 per unit component size, Individual A will experience a fitness cost of 14, giving a total fitness of 25 - 14 = 11, while Individual B will experience a fitness cost of 7, giving a total fitness of 5. Third, an environment is characterized by *Functional Coupling* (*F*), between 0.0 (no functional links between two brain components) and 1.0 (complete functional interdependence between two brain components), which determines how similar brain component benefits are to each other (for *F*=1, all benefits are identical).

The *Evolutionary Process* progresses through the following steps:

1. Determine the number of 'offspring' for each individual in a population, and the age of all individuals, measured in number of generations (these are identical across the population).
2. Initialise an environment and a population of individuals with identical, uniform brain component sizes ($S_{i,j}$ = 1).
3. For a given number of simulation steps
    a. Generate offspring for all individuals
    b. Mutate all offspring
    c. Increase the age of all individuals
    d. Remove individuals whose age exceeds the maximum age
    e. Rank individuals according to their total fitness in the environment (described above)
    f. Remove low-rank individuals until the population size returns to the origin size (i.e. population size is stable over time).

Given the above model parameters, we can examine the effects of developmental coupling (*D*) and functional coupling (*F*) on the evolution of brain component sizes. We can also explore the evolution of brain structure in populations of individuals with an intermediate value of *D* (unless specified otherwise, we use *D*=0.5), which are neither fully-concerted nor fully-mosaic. We call these 'partially-mosaic' individuals, where some of the mutations affect total brain size, scaling each component equally, and some affect each component independently, as given by equation (1) above. We can then assess which strategy, a fully mosaic brain (*D*=0), a fully concerted brain (*D*=1), or a partially-mosaic brain (*D*=0.5), is most successful in different scenarios by measuring the frequency of individuals in a population with that strategy, as a proportion of total population size, after *n* generations. Finally, we can also allow the environment to change randomly over the course of a simulation to examine how temporal heterogeneity in selection regimes affects the long-term success of alternative brain models. The code files in which the model is implemented are available from github.com/shaharavin/BrainEvolutionSimulator. Biplots were made using PlotsOfData (34). Many simulations produce a bimodal distribution of frequencies, we therefore display the mean of these iterations solely to illustrate the skew in the outcome.

ii) Model comparisons

We conducted a series of simulations to explore four key questions identified in the introduction:

1. What mechanisms can produce concerted evolution? Here we fixed *C* and *B* while varying *D*. We then ran the simulation to examine the probability of obtaining coordinated changes in brain components under high, moderate and low levels of *F.*
2. How do costs of brain components affect the way brains respond to selection? Here we fix *F* and *B*, and vary *C* under a range of conditions. Our aim was to test whether the costs of additional brain tissue alter the probability of obtaining a mosaic or concerted brain.
3. How does heterogeneity in fitness affect the way brains respond to selection? Here we fix *F* and *C,* and vary *B* for each brain component under a range of conditions. Our aim was to test whether different levels of heterogeneity in the fitness contribution of additional brain tissue alter the probability of obtaining a mosaic or concerted brain.
4. In a fluctuating environment do strong developmental constraints evolve or collapse? In our final comparison we took a different approach. We introduced a starting population of brains with a range of component sizes and *D*. We then allowed *C* and *B* to vary randomly every 2 generations to test what combination of factors persist over time. We subsequently explored how varying key life history traits (numbers of offspring and maximum age) might buffer the effects of random environmental fluctuation

In each case, the simulation was run over 100 generations, with 1000 iterations, a fixed population size of 300 individuals, initiated with 100 individuals per *D*-strategy. In the main text we present results of simulations with a mutation step size of 5%, but models were also run with a larger mutation step size of 50% to examine how effects were influenced by mutation size. To explore the early stages of the simulations, we also present results from a subset of simulations with 10 generations. In experiments 2 and 3 simulations were run with an initial population containing equal numbers of individuals with different *D*-strategies (*D*=0, 0.5 or 1), which were then evolved under different environment conditions (determined by *F* and the ratio of benefits to cost). In experiment 4, environmental conditions were randomly varied every 2 generations for 150 generations. The 'success' of a *D*-strategy was determined by the proportion of individuals in a population with that strategy at the end of the simulation run. The full output of all models are summarised in Figures S2-S18. The frequency of *D*-strategies were compared using generalised linear models and the glm() function in R (35) across batches of nine, 1000-iteration simulations where *F, D* and *B/C* varied (experiments 1-3, see for example Figures S2,S6), or where *F, D,* maximum lifespan and offspring number varied (experiment 4, see, for example Figures S13) (all experiments total *n*=27,000 iterations). We estimated the effects of all parameters and interactions where indicated, with a Gaussian distribution when comparing 'degrees of mosaicism' (defined as the natural log of the ratio between the largest brain component and the smallest brain component in each individual, averaged across the population) and a quasibinomial distribution when comparing proportional frequencies.

Results

i) Developmental and functional coupling can both produce concerted evolution

By varying the degree of both developmental coupling (*D*), and functional interdependence (*F*), between brain components, our model suggests that patterns of 'concerted' brain evolution, in which the size of brain components vary in tandem, can be caused by both developmental and functional coupling (Figure 1, Figure S2-4). Unsurprisingly, the probability of patterns of concerted evolution declines with decreasing *D* (t=50.330, $p<0.001$; Figure 1D). However, there is a significant interaction between *F* and *D* (t=28.730, $p<0.001$) whereby, for a given value of *D*, where $D < 1$, the probability of concerted evolution increases with higher values of *F* (Figure 1A-C, D), demonstrating that functional interdependence also promotes concertedness. Even when components are completely developmentally independent (*D* is set to 0), high values of *F* can favour comparatively low levels of mosaicism (Figure 1C). Mutation size also has an effect on the

outcome, with more mosaic brains evolving with larger mutation step sizes for a given *D* value (t=133.650, p<0.001; compare Figures S2 and S3). These results suggest macro-evolutionary patterns of allometric scaling consistent with concerted evolution are not, in themselves, sufficient to distinguish between alternative mechanistic models of brain evolution.

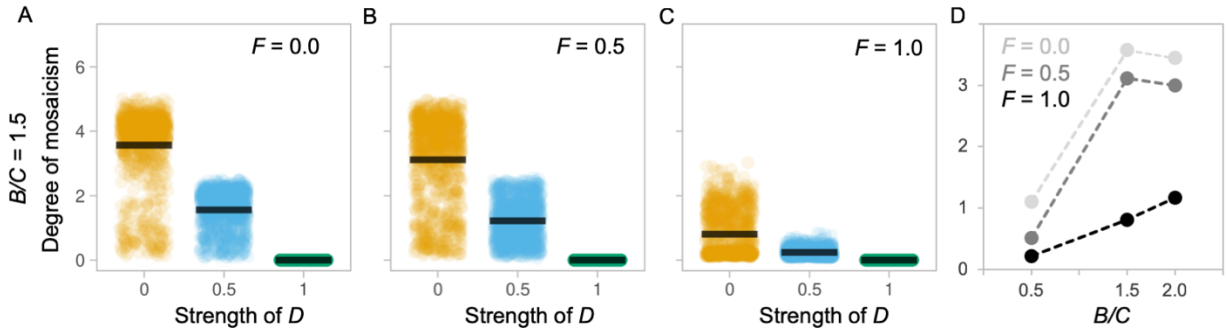

Figure 1: Evolution of 'mosaicism' under alternative conditions. **(A-C)** Each plot depicts the 'degree of mosaicism'' (y-axis, defined as the natural log of the ratio between the largest brain component and the smallest brain component in each individual, averaged across the population) as a function of developmental coupling *D* (x-axis) at the end of a 100-generation simulation run, compiled over 1,000 simulation runs, for a population of 100 individuals with an identical *D*, under different environments, defined by their functional coupling *F*, with a benefit to cost ratio (*B/C*) of 1.5 and a mutation step size of 5%. **(D)** Summary of the effects of varying *F* and *B/C* on the degree of mosaicism. See Figures S2-S4 for full results varying *B/C* and *F*, iteration numbers and mutation step size.

ii) Mosaic and concerted evolution can both be adaptive strategies

By competing alternative *D*-strategies against one another, we found that both *D* (t=21.358, p<0.001) and *F* (t=42.595, p<0.001) affect survival in a particular environment. At an intermediate benefit to cost ratio (*B/C*=1.5) we found that the probability of success of a mosaic, low-*D* strategy increases when *F* is low, while high values of *F* result in a higher probability of success of the concerted, high-*D* strategy (Figure 2A-C; Figure S6-S8). A 'partially-mosaic' strategy (*D*=0.5) is very rarely favoured (Figure 2A-C; Figure S6-S8). These comparisons indicate that variation in the homogeneity of selection across components alters the outcome of competing strategies.

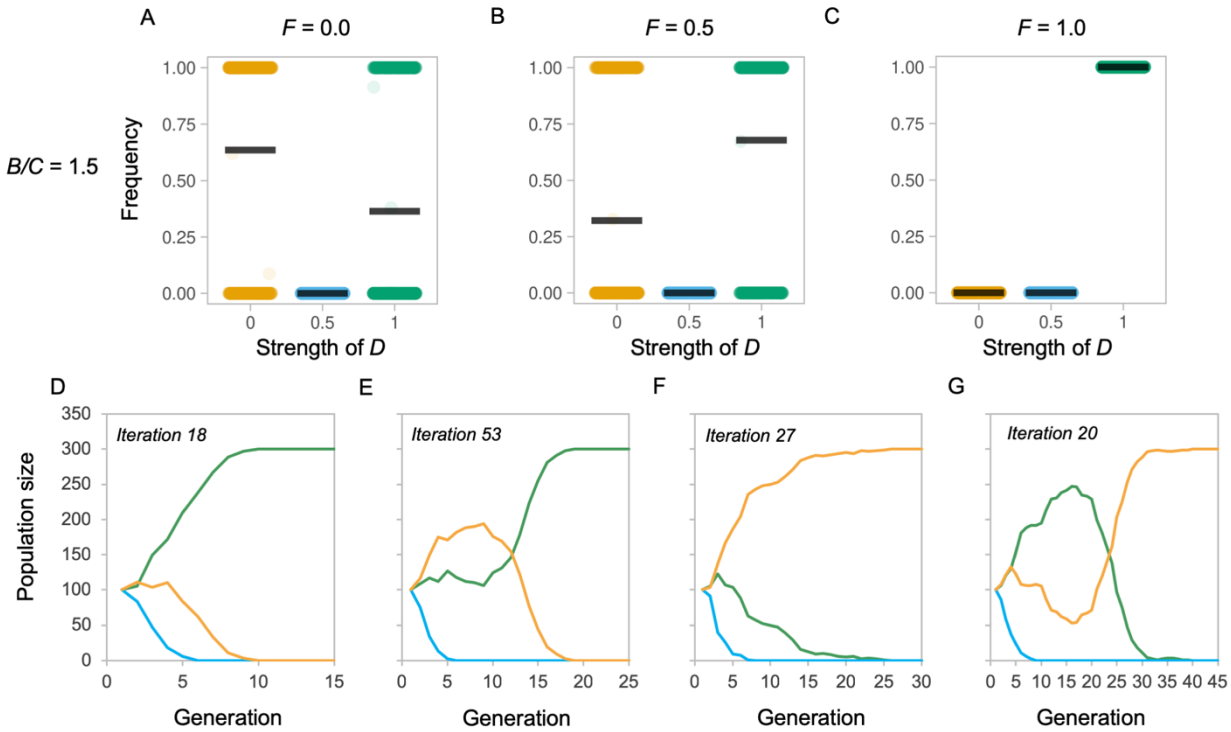

Figure 2: Selected examples of competition between evolving populations with different *D*-strategies. (A-C) Each plot depicts the frequency of that *D*-strategy relative to the total population (y-axis) as a function of developmental coupling *D* (x-axis) at the end of a 100-generation simulation run, compiled over 1,000 simulation runs, under alternative environments defined by their functional coupling *F*, with a benefit to cost ratio (*B/C*) of 1.5 and a mutation step size of 5%. Populations are initialised such that there are 100 fully mosaic individuals (D=0.0), 100 partially-mosaic individuals (*D*=0.5) and 100 concerted individuals (*D*=1.0). (D-G) Selected, representative, individual simulations showing the change in population frequencies over generations for a 5% mutation size and *B/C*=1.5. Colours indicate the *D*-strategy, or *D* value, where yellow is *D*=0, where blue is *D*=0.5, and where green is *D*=0. These show a general pattern of smooth progression from the starting state of equal populations to one strategy winning out (D, F), with only a minority of iterations showing signs of strategies 'swapping' the lead (E,G). This consistency is expected under constant selection regimes. See Figures S6-S8 for full results varying *B/C* and *F*, iteration numbers and mutation step size, and Figures S9-11 for simulations in tailored environments that illustrate parameter effects.

291 ***iii) Costs of additional tissue alter the outcome of competing models***

292 In experiment 1, the degree of mosaicism is also associated with *B/C* ratio (t=131.790, $p<0.001$;
293 Figure 1D, Figure S1), which interacts with *D* (t=-90.970, $p<0.001$) such that the degree of
294 mosaicism tends to increase with *B/C* (Figure 1D). We next repeated the simulations described
295 in (ii) while varying the *B/C* ratio associated with additional brain tissue. The initial models were
296 run with an average *B/C* ratio of 1.5 (Figure 1, Figure S6-8 second row), and were re-run with
297 ratios of 2 and 0.5 (Figure 3A-C, S6-8, first and third rows), simulating low and high costs of brain
298 expansion. This revealed tissue costs have a major effect on the success of competing strategies
299 (t=12.116, $p<0.001$). *B/C* interacts with *D* (t=-13.885, $p<0.001$) such that, for a given combination
300 of *F* and *D*, a high *B/C* (=2) consistently increases the probability of success for the high *D* strategy
301 (Figure 3A-C, Figures S6-S8). In contrast, for a given combination of *F* and *D*, a moderate *B/C*

(=1.5) consistently increases the probability of success for mosaic models. However, when the *B/C* ratio is low (=0.5) the non-linear nature of the interaction between *C, F* and *D* is revealed, such that concertedness again becomes a successful strategy, even at low *F* values (Figure 3D-F, Figure S6-S8 third rows). This can be explained if developmental coupling facilitates rapid *decreases* in all brain regions when costs of brain tissue exceed the benefit, allowing a quick escape from a costly phenotype. To further illustrate these effects, we specified particular parameter comparisons that show how *B/C* interacts with changes in selection regimes such that the most successful strategy switches based on changing the benefit cost ratio (Figures S9-S11 rows) or the homogeneity of selection across components (Figure S9-S11 columns). In particular, we note the relative success of mosaic strategies when one or two components provide a net benefit to size, while other component(s) provide a net cost, while concerted strategies are more favoured when all components provide *either* a net benefit or a net cost. In these competition experiments, mutation size had no effect on the outcome (t=0.740, p=0.459; compare Figures S6 and S7).

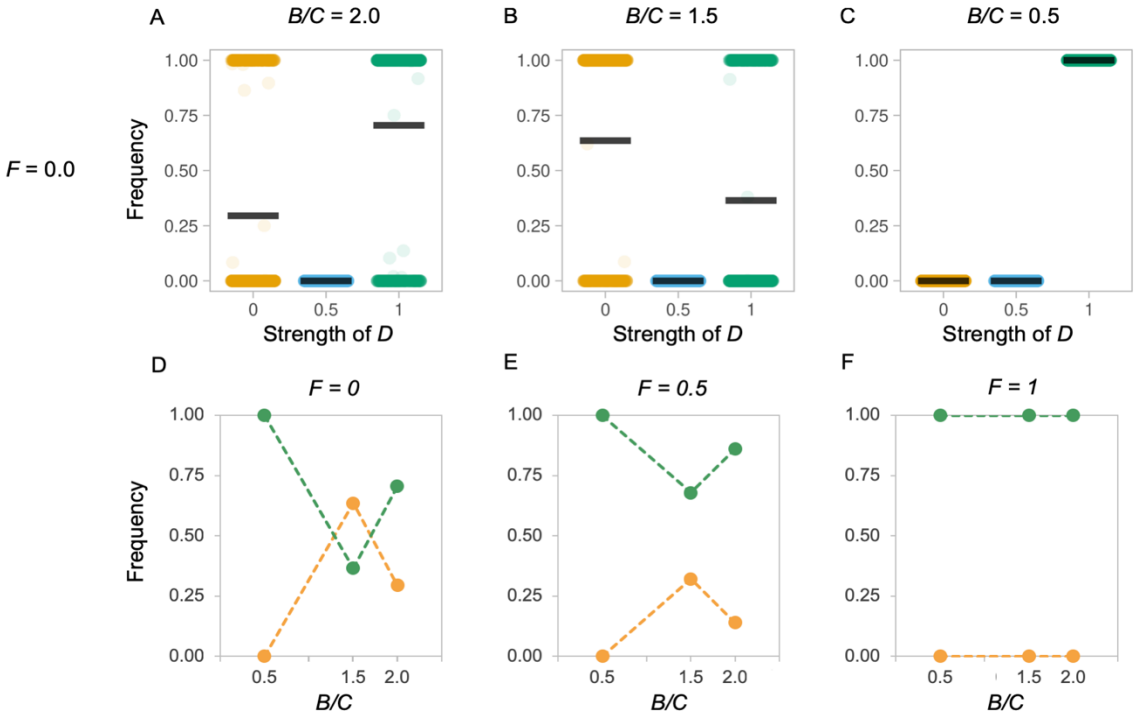

Figure 3: Selected examples of competition between evolving populations with different *D*-strategies, showing the effects of varying the benefit to cost ratio (*B/C*). **(A-C)** Each plot depicts the frequency of that *D*-strategy relative to the total population (y-axis) as a function of developmental coupling *D* (x-axis) at the end of a 100-generation simulation run, compiled over 1,000 simulation runs, with a mutation step size of 5%, and *F*=0 to exemplify the effects of varying the *B/C* from 0 to 2. Populations are initialised such that there are 100 fully mosaic individuals (*D*=0.0), 100 partially-mosaic individuals (*D*=0.5) and 100 concerted individuals (*D*=1.0). (**D-E)** Each plot depicts the average relative frequencies of *D=0* (yellow) and *D=1* (green) at the end of a 1,000 iterations of a 100 generation simulation, at three *B/C* ratios, across three *F* values representing low (**D**), moderate (**E**), and high (**F**) functional coupling. See Figures S6-S8 for full results varying *B/C* and *F*, iteration numbers and mutation step size, and Figures S9-11 for simulations in tailored environments that illustrate parameter effects.

316 ***iv) Variation in the homogeneity of selection across time alters the outcome of competing***
317 ***models but interacts with life history***
318 In a final set of simulations, we examined whether alternative *D*-strategies persist when the
319 selection regime is temporally heterogeneous (due to randomised, independent changes in *B*, *C*
320 and *F*). Under initial conditions, where offspring number was set to 1 and maximum age was set
321 to 3, both concerted and mosaic strategies persist over 150 generations with roughly equal
322 probabilities (Figure 4A). Plotting the frequency of *D*-strategies from individual simulations shows
323 the success of each strategy can fluctuate over time (Figure 4E-G), with multiple *D*-strategies
324 persisting, on average, for 62 generations (Figure S12A). This is substantially more than is found
325 in simulations with fixed environments (Figure S5), and is also reflected in the high average
326 generation at extinction for each *D*-strategy (D=0, 91; D=0.5, 57; D=1, 98; Figure S12). We
327 subsequently varied maximum age and offspring number to explore how 'slow' (long lives, few
328 offspring) or 'fast' (short lives, many offspring) life histories buffer the effects of environmental
329 heterogeneity. This revealed that the main effect captured in the model was that of offspring
330 number interacting with *D* (t=43,622, $p<0.001$), with higher offspring numbers increasing the
331 probability of success of the concerted, high-*D* strategy (Figure 4A,C,D; Figure S13-S15
332 columns). Increasing maximum lifespan had a significant, but smaller effect in the opposite
333 direction (t=-4.349, $p<0.001$; Figure 4A,B,D; Figure S13-S15 rows). Altering the amplitude of
334 fluctuations in the environment also has a subtle effect on the probability of success between
335 competing *D*-strategies (t=-8.986, $p<0.001$), with more extreme conditions slightly increasing the
336 success of concertedness (Figure S18). In these competition experiments, mutation size again
337 had no effect on the outcome (t=1.000, p=1.000; compare Figures S13 and S14).
338
339

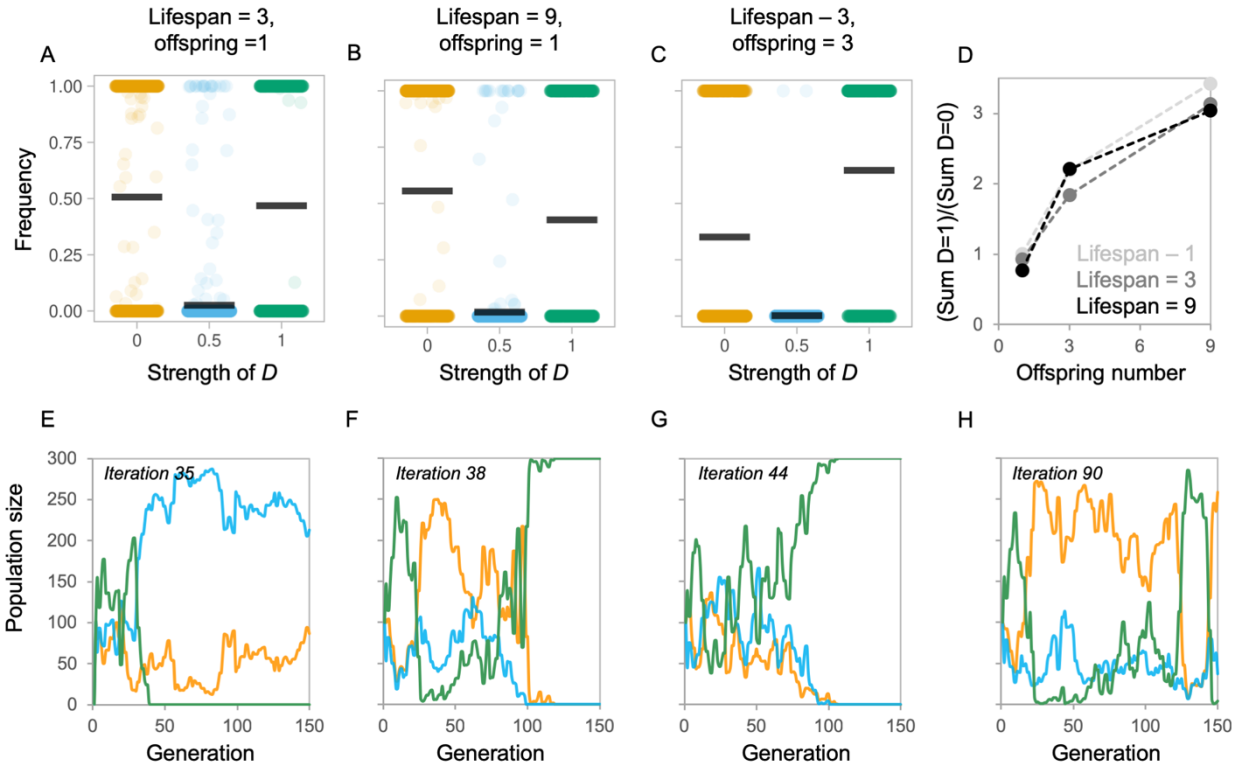

Figure 4: Selected examples of competition between *D*-strategies in a randomly varying environment. **(A-C)** Each plot depicts the ratio of that strategy to the total population (y-axis) as a function of developmental coupling *D* (x-axis) at the end of a 150-generations, compiled over 1,000 simulation iterations; every 2 generations the environment was replaced, using a uniform random distribution for cost [0.5, 5], max average benefit [0.51, 105], and *F* functional coupling [0, 1]. Populations are initialized such that there are 100 fully mosaic individuals (*D*=0.0), 100 partially-mosaic individuals (*D*=0.5) and 100 concerted individuals (*D*=1.0). Simulations were performed varying two life history conditions: maximum lifespan, or the number of generations an individual persists alive, and offspring number, which are produced once every generation. Three combinations of lifespan and offspring are shown, for full comparisons see S13. **(D)** A summary of the ratio of concerted individuals (*D*=1) to mosaic individuals (*D*=0) at the end of each iteration of the 150 generation simulation, showing the effects of maximum lifespan and offspring number. **(E-G)** Selected, representative, individual simulations showing fluctuations in *D*-strategy frequencies over generations. Colours indicate the *D*-strategy, or *D* value, where yellow is *D* =0, where blue is *D*=0.5, and where green is *D*=1. See Figures S13-S16 for full results varying *B/C* and *F*, iteration numbers and mutation step size, and S17 for effects of increasing the size of environmental fluctuations.

340

341

342

343

344

345

346

347

Discussion

The results of our agent-based simulations have several implications for studies using comparative volumetric data to interrogate mechanistic hypotheses of how brains evolve. First, they demonstrate that patterns of 'concerted' evolution (consistent allometric scaling of all brain components across macroevolutionary time) should not be taken as evidence for developmental coupling, as concertedness can also evolve due to high functional interdependence in the absence of developmental coupling. Second, the most probable route to adaptive brain evolution is strongly influenced by whether the change in selection regime is skewed towards one brain component or i s evenly distributed across the whole brain, and what the relative costs and benefits of increased investment in brain tissue are. Third, depending on context, both concerted and mosaic evolution can be adaptive strategies. Finally, we suggest temporal variation in selection regimes can result in both strategies being maintained in a population. Given these results, pluralism is a tempting settlement. However, this ecumenism opens new questions: Under what conditions do developmental coupling and un-coupling succeed? What causes switches between mosaic and concerted modes of evolution? And how can we empirically distinguish them?

i) Concertedness is a phenotypic pattern devoid of mechanistic information

Our simulations clearly show that concerted brain evolution can occur under any of our *D*-strategies (Figure 1). The probability of concertedness predictably increases with *D,* but it also increases with *F*, even when *D* is zero. Why do high *F* values result in concerted evolution? If we assume that selection acts on specific brain components, and excess brain tissue is generally expensive, then selection to maintain functional relationships should be expected, and would result in co-evolution among brain components. These formal results are consistent with empirical data. First, across mammals the major components of the visual processing pathway, including the peripheral visual system, lateral geniculate nucleus and visual cortex, tend to co-evolve with one another, as predicted by their functional integration (36-38). Similarly, major components of the olfactory pathway, including the olfactory bulbs and olfactory cortex, also co-evolve (36,39). However, the visual and olfactory pathways show no consistent pattern of co-evolution between them (36). Indeed, whether they co-vary negatively, positively, or not at all, can be explained by how diet and activity pattern interact to shape foraging behaviour (36). Second, major brain structures connected by long-range axons, such as the neocortex and cerebellum also tend to co-evolve independently of total brain size, while also showing evidence of temporally transient

independent change (40-44). Finally, our model demonstrates an interaction between *D* and *F*, which may suggest that a pattern of concertedness driven by *F* could select for, or against, developmental integration. Regardless, our results demonstrate that concerted patterns of brain evolution provide no evidence either for or against the prevalence of developmental coupling.

ii) The costs and benefits of brain tissue, and the complexity of the mutation landscape

Our simulations suggest that the cost of excess brain tissue and the distribution of selection across networks of brain components play critical roles in determining how brains evolve. When the strength and direction of selection is skewed towards one brain component, the probability that a mosaic, low-*D* strategy will be successful is increased. However, when the relative costs of neural tissue are either very low or high, the balance can switch to favour a high-*D* strategy. This likely reflects the 'speed' at which the two populations can respond to selection. With only one mutational mechanism, it is potentially more likely for a developmentally coupled brain to evolve towards a new 'adaptive peak' than it is for a mosaic brain. This is because the mutational landscape for a mosaic brain is more complex, and the probability of hitting the optimal mutational path is reduced by a greater number of potential mutational outcomes. At face value, our simulations therefore support previous arguments that "…a coordinated enlargement of many independent components of one functional system without enlargement of the rest of the brain may be more difficult, as its probability would be the vanishingly small product of the probability of each component enlarged individually" (2, p 1583). However, if the costs of brain components are unequal, as may be expected if energetic consumption scales with neuron number (33) and neuron density varies between components (45-47), then this effect would be dampened according to the distribution of costs and benefits across the whole system. Hence, an uneven distribution of neural costs would likely increase the probability of mosaicism. Evidence that this effect occurs in nature may be provided by recent data showing life history traits constrain specific brain regions independently of overall brain size (48).

While accurately assessing the fitness costs and benefits of brain tissue remains challenging, we suggest some tentative predictions based on these interpretations. First, we expect mosaicism to be less likely during transitions to high quality diets, as the cost of neural tissue relative to the overall energy budget may be reduced. Second, under sudden periods of energy resource limitation brains should shrink, at least initially, in a concerted manner. Third, mosaicism may be more likely when energy intake is relatively constant, but selection favours changes in neural investment which involve energetic trade-offs. This may be common during

periods of ecological change that are not associated with changes in body size (and by proxy energetic intake), or in taxa that are size limited.

iii) Partially-mosaic brains and the maintenance of diversity

It may be surprising that partially-mosaic individuals, which are seemingly a compromise-state, generally have low probability of success in our simulations. This can again be explained by the 'cost' of mutation. In short, partially-mosaic individuals incur the highest cost of mutational complexity. If the direction of mutation is random, in a given generation the partially-mosaic brain simply has lower odds of increasing its fitness because mutations affecting whole brain and region-specific size may often be in conflict. The relative lack genetic variation contributing to both whole brain and region specific size in natural populations (5,18,25) is in keeping with this conclusion. However, how mutational effects interact during brain development requires further investigation.

However, our simulations across heterogeneous selection regimes indicate that alternative *D*-strategies can persist within a single population for many generations. This provides an alternative route to mixed temporal patterns of concerted and mosaic evolution within a single population. If we view *D*-strategies in our model as alternative genotypes, this implies that genetic variation affecting specific components or total brain size may both either persist at low levels in natural populations, or periodically arise *de novo* and spread through a population. Regardless, this would enable selection to fluctuate between favouring mosaic and concerted mechanisms, permitting both adaptive restructuring and adaptive conservation of brain structure.

iv) Reconciling mosaic and concerted views

Our simulation results suggest a way of reconciling mosaic and concerted views of brain evolution. Developmentally coupled brains evolve in scenarios involving some combination of tissue costs being evenly distributed, and an extreme and variable fitness landscape, while mosaic brains are the result of environmental stability coupled with differentiated selection among components. The quick evolutionary response enabled by developmentally coupled brain evolution makes it ideal for circumstances where getting it 'approximately correct', quickly is advantageous, while mosaic evolution is favoured when accuracy trumps speed. This is also tied to life-history and environmental heterogeneity. For example, large offspring number, which increases short term competition, favours the fast response provided by developmental coupling, while lower competition allows mosaic strategies to persist, find the optimum brain structure, and out-compete developmentally coupled individuals.

The contrasting benefits of concerted and mosaic strategies brings us back to a major initial division between the two hypotheses (1,12,14), which continues to be widely reported in the literature (e.g. 5-11); where developmental coupling does occur, is it a constraint, or has it evolved and is therefore *evolvable*? Our simulations support developmental coupling as a scenario-dependent adaptive strategy, rather than a constraint. First, our simulations show that the fate of the two opposing strategies can vary through time. In nature, this would be reflected in the formation and breaking of genetic correlations between traits. Second, the general absence of genetic correlations observed in quantitative genetics studies is reconciled with concertedness via developmental coupling by invoking the importance of *de novo* mutation, but our simulations suggest that the probability that these mutations will spread to fixation depends on the environmental context. By showing that the distribution and size of costs and benefits are critical in determining the outcome of competing strategies, our model supports a view whereby global selection regimes determine the constraints acting on brain evolution, not the developmental program. Two key conclusions from this work are therefore i) patterns of concertedness should not be equated with developmental coupling, and ii) developmental coupling should not be equated to developmental constraint.

v) Conclusions

In sum, our agent-based simulations of competing views of brain evolution provide a number of informative predictions that should refresh our view of this ongoing debate. First, we show concertedness is an outcome, not a mechanism. Second, we demonstrate that selection regime and structural interdependencies are critical to the outcome of competing strategies. Third, we argue that both developmentally coupled and uncoupled brain architectures can both represent adaptive strategies, but we contest the assumption that developmental coupling is necessarily a persistent evolutionary constraint. Finally, our model provides a way to integrate patterns of brain evolution, life history and environmental heterogeneity. We of course acknowledge that our model is a simplification of a highly complex biological phenomenon. While the assumptions we make in constructing the model are intended to help us clearly explore previous verbal arguments, several extensions are possible. These include the addition of heterogeneous distributions of energetic costs, costs of functional integration to mirror energetic costs of long-range axon, and a total brain size ceiling imposed by allometric scaling with body size, which is itself under selection. Constraints imposed by brain~body co-evolution are of particular interest, as they may, for example, limit energetic investments in brain tissue, increasing the strength of trade-offs between components. This could alter the outcome of competition between *D*-strategies. Nevertheless, we

hope the general approach taken can trigger greater formalisation of evolutionary hypotheses in this field, and work that further refines our computational models.

Acknowledgements

We thank Corina Logan, for instigating this collaboration, the Castiglione family for facilitating discussions, and two anonymous reviewers for very constructive comments and advice.

Funding

AC was supported by the Templeton World Charity Foundation (TWCF0303). SHM was supported by a NERC Independent Research Fellowship (NE/N014936/1).

Author contributions

SA, AC and SHM devised the model, interpreted the output and wrote the manuscript. SA produced the code to implement the model.

References

1. Finlay BL, Darlington RB, Nicastro N. 2001. Developmental structure in brain evolution. Brain Behav Sci. 24:298–304. DOI: 10.1017/S0140525X01003958Published
2. Finlay B, Darlington R. 1995. Linked regularities in the development and evolution of mammalian brains. Science 268(5217):1578–84. DOI: 10.1126/science.7777856
3. Yopak KE, Lisney TJ, Darlington RB, Collin SP, Montgomery JC, Finlay BL. 2010. A conserved pattern of brain scaling from sharks to primates. Proc Natl Acad Sci. 107(29):12946–51. DOI: 10.1073/pnas.1002195107
4. Workman AD, Charvet CJ, Clancy B, Darlington RB, Finlay BL. 2013. Modeling transformations of neurodevelopmental sequences across mammalian species. J Neurosci. 33(17):7368–83. DOI: 10.1523/JNEUROSCI.5746-12.2013
5. Hager R, Lu L, Rosen GD, Williams RW. 2012. Genetic architecture supports mosaic brain evolution and independent brain–body size regulation. Nat Commun 3(1). DOI: 10.1038/ncomms2086
6. Striedter GF. 2005. Principles of brain evolution. Oxford: Sinaur Associates.
7. Gutiérrez-Ibáñez C, Iwaniuk AN, Moore BA, Fernandez-Juricic E, Corfield JR, Krilow JM, Kolominsky J, Wylie DR. 2014. Mosaic and concerted evolution in the visual system of birds. *PLoS One* 9(3). DOI: 10.1371/journal.pone.0090102

8. Noreikiene K, Herczeg G, Gonda A, Balázs G, Husby A, Merilä J. 2015. Quantitative genetic analysis of brain size variation in sticklebacks: support for the mosaic model of brain evolution. Proc R Soc B 282(1810):20151008. DOI: 10.1098/rspb.2015.1008
9. Kotrschal A, Zeng HL, van der Bijl W, Öhman-Mägi C, Kotrschal K, Pelckmans K, Kolm N. 2017. Evolution of brain region volumes during artificial selection for relative brain size. Evolution, 71(12): 2942-2951.DOI: 10.1111/evo.13373
10. Sukhum KV, Shen J, Carlson BA. 2018. Extreme enlargement of the cerebellum in a clade of teleost fishes that evolved a novel active sensory system. Current Biol 28(23): 3857-3863. DOI: 10.1016/j.cub.2018.10.038
11. D'Aniello B, Di Cosmo A, Scandurra A, Pinelli C. 2019. Mosaic and concerted brain evolution: the contribution of the microscopic comparative neuroanatomy in lower vertebrates. Front Neuroanat 13: 86. DOI: doi.org/10.3389/fnana.2019.00086
12. Harvey P, Krebs JR. 1990. Comparing brains. Science 13;249(4965):140–6. DOI: 10.1126/science.2196673
13. Huber R, van Staaden MJ, Kaufman LS, Liem KF. 1997. Microhabitat use, trophic patterns, and the evolution of brain structure in African cichlids. Brain, Behav Evol 50(3); 167-182. DOI: 10.1159/000113330
14. Barton RA, Harvey PH. 2000. Mosaic evolution of brain structure in mammals. Nature 405:4. DOI: 10.1038/35016580
15. Iwaniuk AN, Dean KM, Nelson JE. 2004. A mosaic pattern characterizes the evolution of the avian brain. Proc R Soc B. 271 (suppl 4): S148-S151. DOI: 10.1098/rsbl.2003.0127
16. Willemet R. 2012. Understanding the evolution of mammalian brain structures; the need for a (new) cerebrotype approach. Brain Sci. 2(2):203–24. DOI: 10.3390/brainsci2020203
17. Montgomery SH, Mundy NI, Barton RA. 2016. Brain evolution and development: adaptation, allometry and constraint. Proc R Soc B. 283(1838):20160433. DOI: 10.1098/rspb.2016.0433
18. Godfrey-Smith P. Complexity and the function of mind in nature. New York: Cambridge University Press; 1996.
19. Brown WM. Natural selection of mammalian brain components. 2001. Trends Ecol Evol. 16(9):471–3. DOI: 10.1016/S0169-5347(01)02246-7
20. Charvet CJ, Darlington RB, Finlay BL. 2013. Variation in human brains may facilitate evolutionary change toward a limited range of phenotypes. Brain Behav Evol. 81(2):74–85. DOI: 10.1159/000345940
21. Beatty J. 1997. Why do biologists argue like they do? Philos Sci. 64:S432–43. DOI: 10.1086/392620
22. Barton RA. 2001. The coordinated structure of mosaic brain evolution. Behav Brain Sci. 24:281–2.
23. Deaner RO, van Schaik CP. 2001. Flaws in evolutionary theory and interpretation. Behav Brain Sci. 24:279–80.
24. Airey DC, Williams RW. 2001. Quantitative neurogenetic perspectives. Brain Behav Sci. (24):282–3.

25. Henriksen R, Johnsson M, Andersson L, Jensen P, Wright D. 2016. The domesticated brain: genetics of brain mass and brain structure in an avian species. Sci Rep 6(1). DOI: 10.1038/srep34031
26. Parke EC. 2014. Experiments, simulations, and epistemic privilege. Philos Sci. 81(4):516–36. DOI: 10.1086/677956
27. González-Forero M, Faulwasser T, Lehmann L. 2017. A model for brain life history evolution. PLOS Comput Biol. 13(3):e1005380. DOI: 10.1371/journal.pcbi.1005380
28. González-Forero M, Gardner A. 2018. Inference of ecological and social drivers of human brain-size evolution. Nature 557(7706):554–7. DOI: 10.1038/s41586-018-0127-x
29. dos Santos M, West SA. 2018. The coevolution of cooperation and cognition in humans. Proc R Soc B. 285(1879):20180723. DOI: 10.1098/rspb.2018.0723
30. Muthukrishna M, Doebeli M, Chudek M, Henrich J. 2018. The cultural brain hypothesis: how culture drives brain expansion, sociality, and life history. PLOS Comput Biol. 14(11):e1006504. DOI: 10.1371/journal.pcbi.1006504
31. Dunbar RIM. 2001. Confounding explanations.... Brain Behav Sci. 24:283.
32. Striedter GF. 2001. Brain evolution: How constrained is it? Behav Brain Sci. 24:296–7.
33. Herculano-Houzel S. 2011. Scaling of brain metabolism with a fixed energy budget per neuron: implications for neuronal activity, plasticity and evolution. PLoS ONE 6(3):e17514. DOI: 10.1371/journal.pone.0017514
34. Postma M, Goedhart J. 2019. PlotsOfData—A web app for visualizing data together with their summaries. PLOS Biol. 17(3):e3000202. DOI: 10.1371/journal.pbio.3000202
35. R Core Team (2013). R: A language and environment for statistical computing. https://www.r-project.org
36. Barton RA. 1995. Evolutionary radiation of visual and olfactory brain systems in primates, bats and insectivores. Philos Trans R Soc Lond B Biol Sci. 348(1326):381–92. DOI: 10.1098/rstb.1995.0076
37. Barton RA. 1998. Visual specialization and brain evolution in primates. Proc Roy Soc B 265(1409): 1933-1937. DOI: 10.1098/rspb.1998.0523
38. Barton RA. 2004. Binocularity and brain evolution in primates. Proc Natl Acad Sci 101.27: 10113-10115. DOI: 10.1073/pnas.0401955101
39. Barton RA. 2006. Olfactory evolution and behavioral ecology in primates. Am J Primatol 68.6: 545-558. DOI: doi.org/10.1002/ajp.20251
40. Whiting BA, Barton RA. 2003. The evolution of the cortico-cerebellar complex in primates: anatomical connections predict patterns of correlated evolution. J Hum Evol 44(1): 3-10. DOI: 10.1016/S0047-2484(02)00162-8
41. Herculano-Houzel S. 2010. Coordinated scaling of cortical and cerebellar numbers of neurons. *Front Neuroanat 4*, 12. DOI: 10.3389/fnana.2010.00012

589 42. Smaers JB, Steele J, Zilles K. 2011. Modeling the evolution of cortico-cerebellar systems in
590 primates. Annals NY Acad Sci 1225(1): 176-190. DOI: 10.1111/j.1749-6632.2011.06003.x
591 43. Barton RA, Venditti C. 2014. Rapid evolution of the cerebellum in humans and other great
592 apes. Curr Biol, 24(20): 2440-2444. DOI: 10.1016/j.cub.2014.08.056
593 44. Muller AS, Montgomery SH. 2019. Co-evolution of cerebral and cerebellar expansion in
594 cetaceans. J Evol Biol. 32(12): 1418-1431. 10.1111/jeb.13539
595 45. Olkowicz S, Kocourek M, Lučan RK, Porteš M, Fitch WT, Herculano-Houzel S, et al. 2016. Birds
596 have primate-like numbers of neurons in the forebrain. Proc Natl Acad Sci. 113(26):7255–60. DOI:
597 10.1073/pnas.1517131113
598 46. Herculano-Houzel S, Collins CE, Wong P, Kaas JH. 2007. Cellular scaling rules for primate brains.
599 Proc Natl Acad Sci. 104(9):3562–7. DOI: 10.1073/pnas.0611396104
600 47. Herculano-Houzel S, Catania K, Manger PR, Kaas JH. 2015. Mammalian brains are made of these:
601 a dataset of the numbers and densities of neuronal and nonneuronal cells in the brain of glires,
602 primates, scandentia, eulipotyphlans, afrotherians and artiodactyls, and their relationship with body
603 mass. Brain Behav Evol. 86(3–4):145–63. DOI: 10.1159/000437413
604 48. Powell LE, Barton RA, Street SE. 2019. Maternal investment, life histories and the evolution of brain
605 structure in primates. Proc R Soc B Biol Sci. 286(1991):20191608. DOI: 10.1098/rspb.2019.1608
606

An agent-based model clarifies the importance of functional and developmental integration in shaping brain evolution

Shahar Avin[1], Adrian Currie[2#] & Stephen H. Montgomery[3#]

[1] Centre for the Study of Existential Risk, University of Cambridge

[2] Department of Sociology, Philosophy and Anthropology, University of Exeter

[3] School of Biological Sciences, University of Bristol

[#]contributed equally

List of supplementary figures

Figure S1: A simplified, pictorial depiction of the model. Pages 4-5.

Figure S2: Evolution of 'mosaicism' under alternative conditions, full comparisons, run with 5% mutation size and 100 generations [sister to Figure 1]. Page 6.

Figure S3: Evolution of 'mosaicism' under alternative conditions, full comparisons, run with 50% mutation size and 100 generations [extension of Figure 1]. Page 7.

Figure S4: Evolution of 'mosaicism' under alternative conditions, full comparisons, run with 50% mutation size and 10 generations [extension of Figure 1]. Page 8.

Figure S5: Generation number at convergence during simulations of competition between evolving populations with different *D*-strategies under alternative conditions [companion to Figure 2]. Page 9.

Figure S6: Competition between evolving populations with different *D*-strategies under alternative conditions, full comparisons, run with 5% mutation size and 100 generations [sister to Figure 2]. Page 10.

Figure S7: Competition between evolving populations with different *D*-strategies under alternative conditions, full comparisons, run with 50% mutation size and 100 generations [extension of Figures 2 and 3]. Page 11.

Figure S8: Competition between evolving populations with different *D*-strategies under alternative conditions, full comparisons, run with 50% mutation size and 10 generations [extension of Figures 2 and 3]. Page 12.

Figure S9: Competition between evolving populations with different *D*-strategies under tailored environmental conditions, full comparisons, run with 5% mutation size and 100 generations [extension of Figures 2 and 3]. Page 13.

Figure S10: Competition between evolving populations with different *D*-strategies under tailored environmental conditions, full comparisons, run with 50% mutation size and 100 generations [extension of Figures 2 and 3]. Page 14.

Figure S11: Competition between evolving populations with different *D*-strategies under tailored environmental conditions, full comparisons, run with 50% mutation size and 10 generations [extension of Figures 2 and 3]. Page 15.

Figure S12: Conditions at convergence of simulations of competition between evolving populations with different *D*-strategies in a randomly varying environment, under different life history conditions [companion to Figure 2]. Page 16.

Figure S13: Competition between evolving populations with different *D*-strategies in a varying environment, under different life history conditions, full comparisons, run with 5% mutation size and 100 generations [sister to Figure 4]. Page 17.

Figure S14: Competition between evolving populations with different *D*-strategies in a varying environment, under different life history conditions, full comparisons, run with 50% mutation size and 100 generations [extension of Figure 4]. Page 18.

Figure S15: Competition between evolving populations with different *D*-strategies in a varying environment, under different life history conditions, full comparisons, run with 50% mutation size and 10 generations [extension of Figure 4]. Page 19.

Figure S16: Selected, representative, individual simulations showing fluctuations in population frequencies over generations for a 5% mutation size (A-D) or a 50% mutation size (E-H) [extension of Figure 4]. Page 20.

Figure S17: Subtle effects of the size of environmental fluctuations on competition between evolving populations with different *D*-strategies in a varying environment [extension of Figure S16]. Page 21.

Figure S18: Relationship between population frequencies between partially mosaic brains (D=0.5) and fully mosaic (D=0), or concerted brains (D=1) from simulations in varying environmental conditions and a 5% mutation size (A) or 50% mutation size (B) [extension of Figure 4]. Page 22.

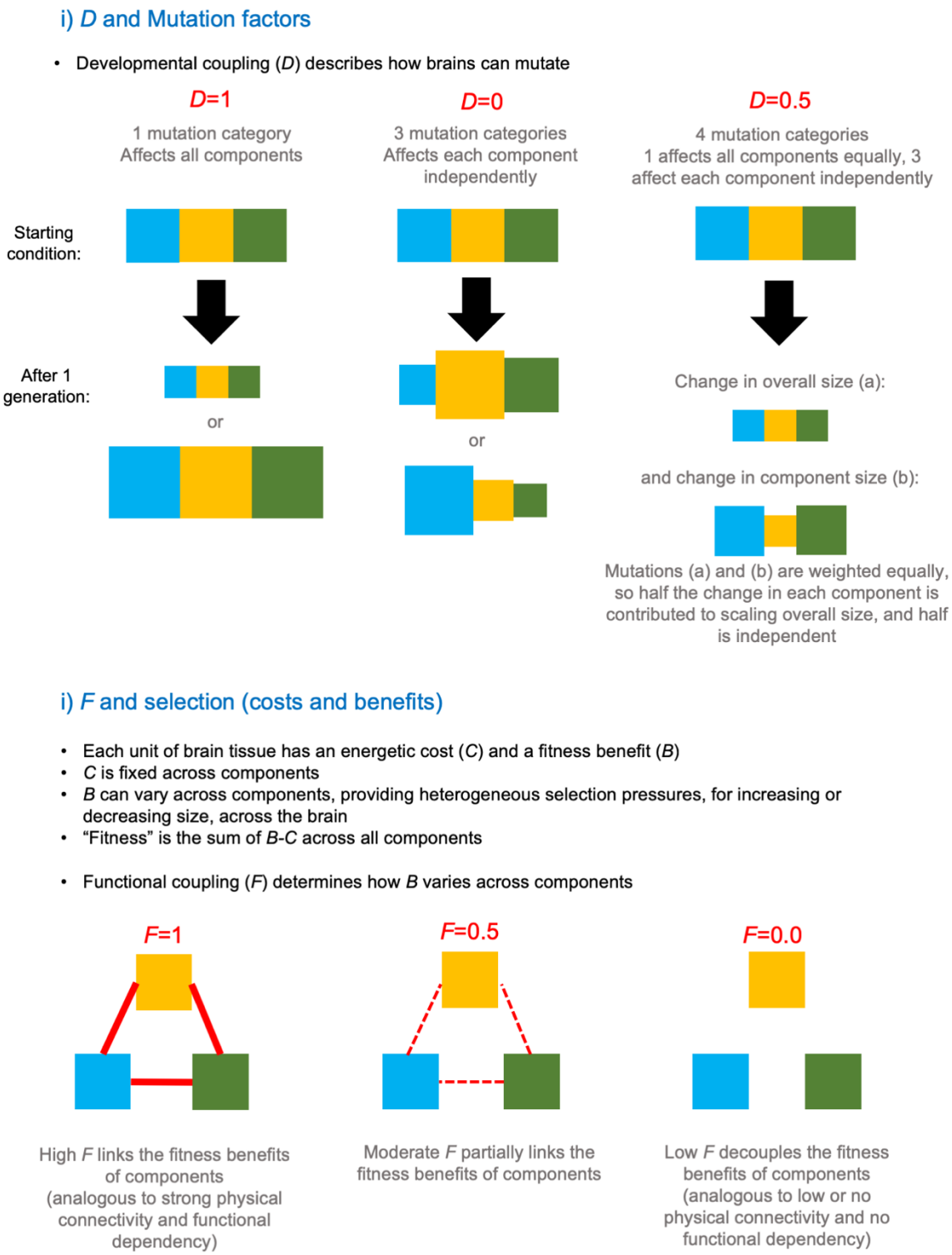

Figure S1: A simplified, pictorial depiction of the model.

iii) Life history of a strategy

- Each individual lives for a set number of generations
- Each individual breeds once a set number of generations, producing a set number of offspring
- Generations can overlap

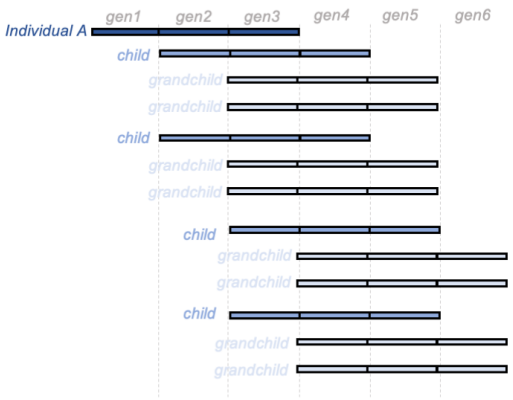

e.g. a population derived from Individual A living for 3 generations, with each individual producing 2 offspring per generation after 1 generation to reach maturity. Great-grandchildren not shown for clarity.

- Population size is kept constant, meaning excess individuals are culled each generation, see (iv) for details.
- This creates 'competition' between strategies with selection determined by the environment imposed by the distribution of *B* across components

iv) Selection and population turnover

- Each individual produces a set number of offspring each of which are 'mutated', as described in (i)
- Variation in overall brain size, and the size of each brain component creates variation in 'fitness' (see ii)
- At each generation, all the individuals are ranked by their 'fitness'

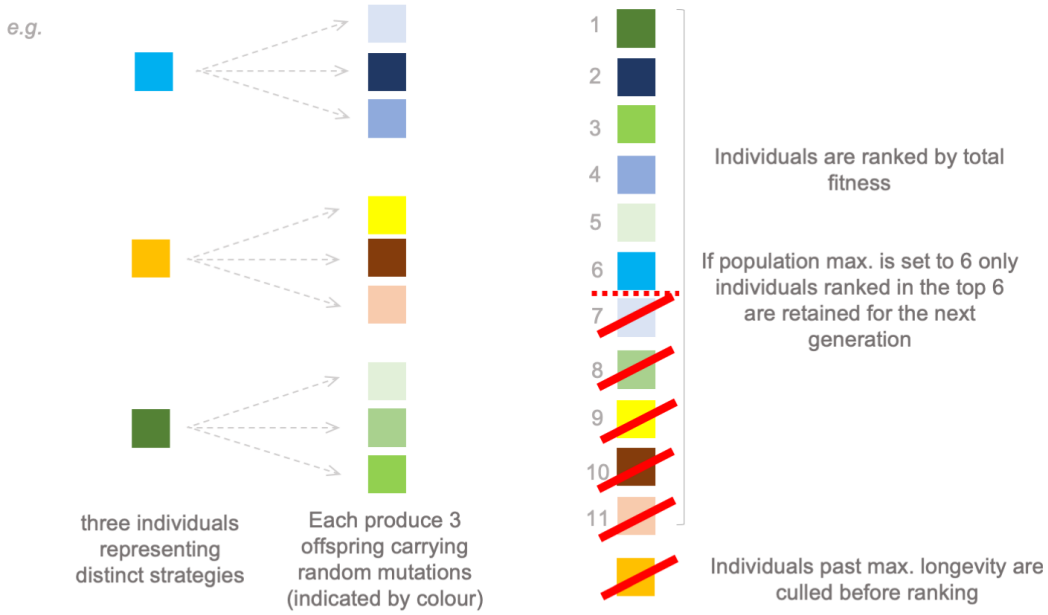

- This process is repeated across a set number of generations. From a starting point of equal representation of strategies, the change in the frequency of a strategy indicates its selective advantage.

Figure S1 cont'd: A simplified, pictorial depiction of the model.

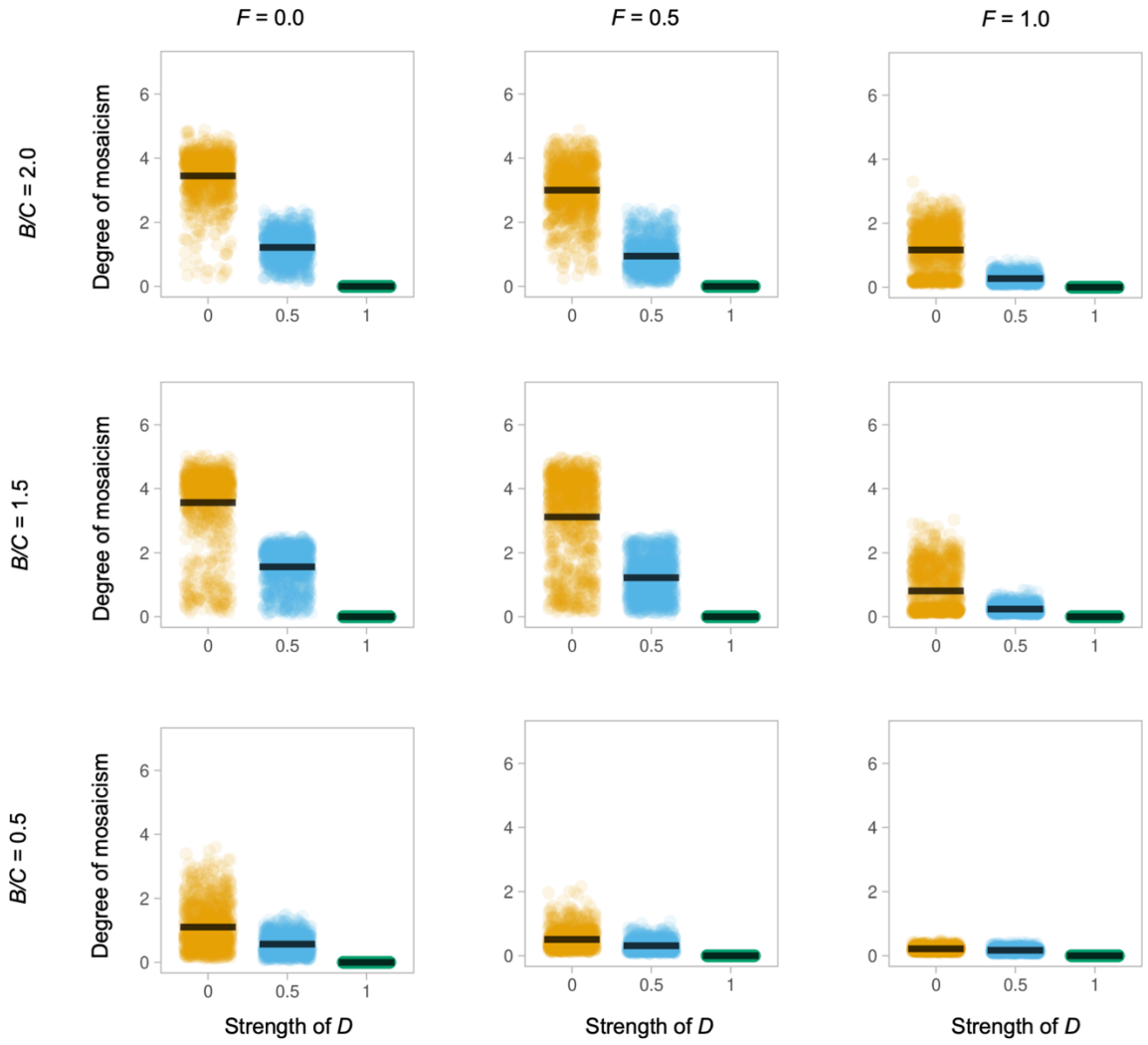

Figure S2: Evolution of 'mosaicism' under alternative conditions, with a mutation step size of 5%. Each plot depicts the 'degree of mosaicism' (y-axis, defined as the natural log of the ratio between the largest brain component and the smallest brain component in each individual, averaged across the population) as a function of developmental coupling *D* (x-axis) at the end of a 100-generation simulation run, compiled over 1,000 simulation runs, for a population of 100 individuals with an identical *D*, under different environments, defined by their functional coupling *F*, and their average benefit to cost ratio [sister to Figure 1].

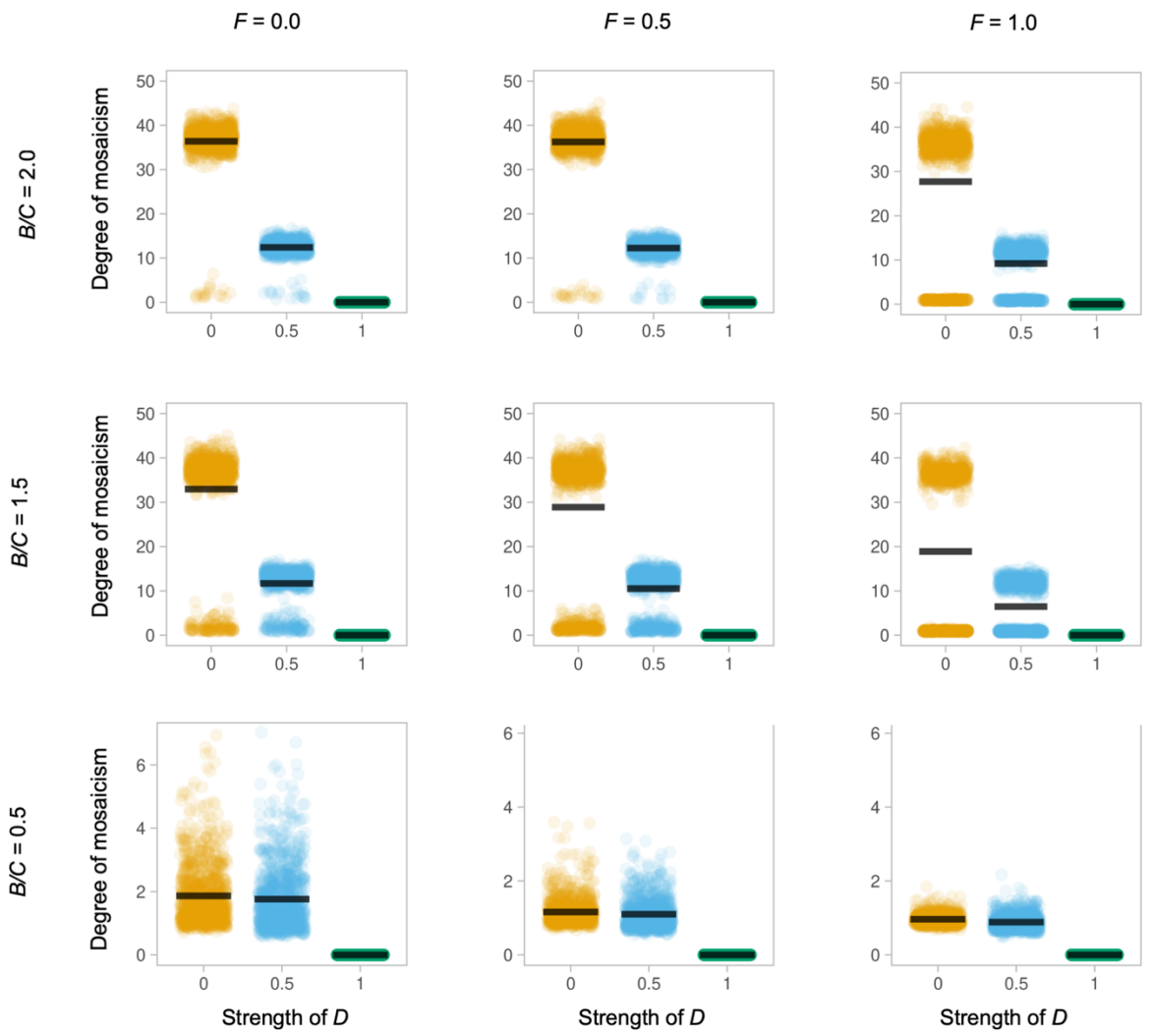

Figure S3: Evolution of 'mosaicism' under alternative conditions, with a mutation step size of 50%. Each plot depicts the 'degree of mosaicism' (y-axis, defined as the natural log of the ratio between the largest brain component and the smallest brain component in each individual, averaged across the population) as a function of developmental coupling *D* (x-axis) at the end of a 100-generation simulation run, compiled over 1,000 simulation runs, for a population of 100 individuals with an identical *D*, under different environments, defined by their functional coupling *F*, and their average benefit to cost ratio. Interestingly our model predicts a step change in levels of mosaicism under some scenarios (e.g. row 2), which can be attributed to the mutational effect size (compare with row 2 in Figure S2). This implies large effect mutations could allow rapid 'jumps' in mosaicism. [extension of Figure 1].

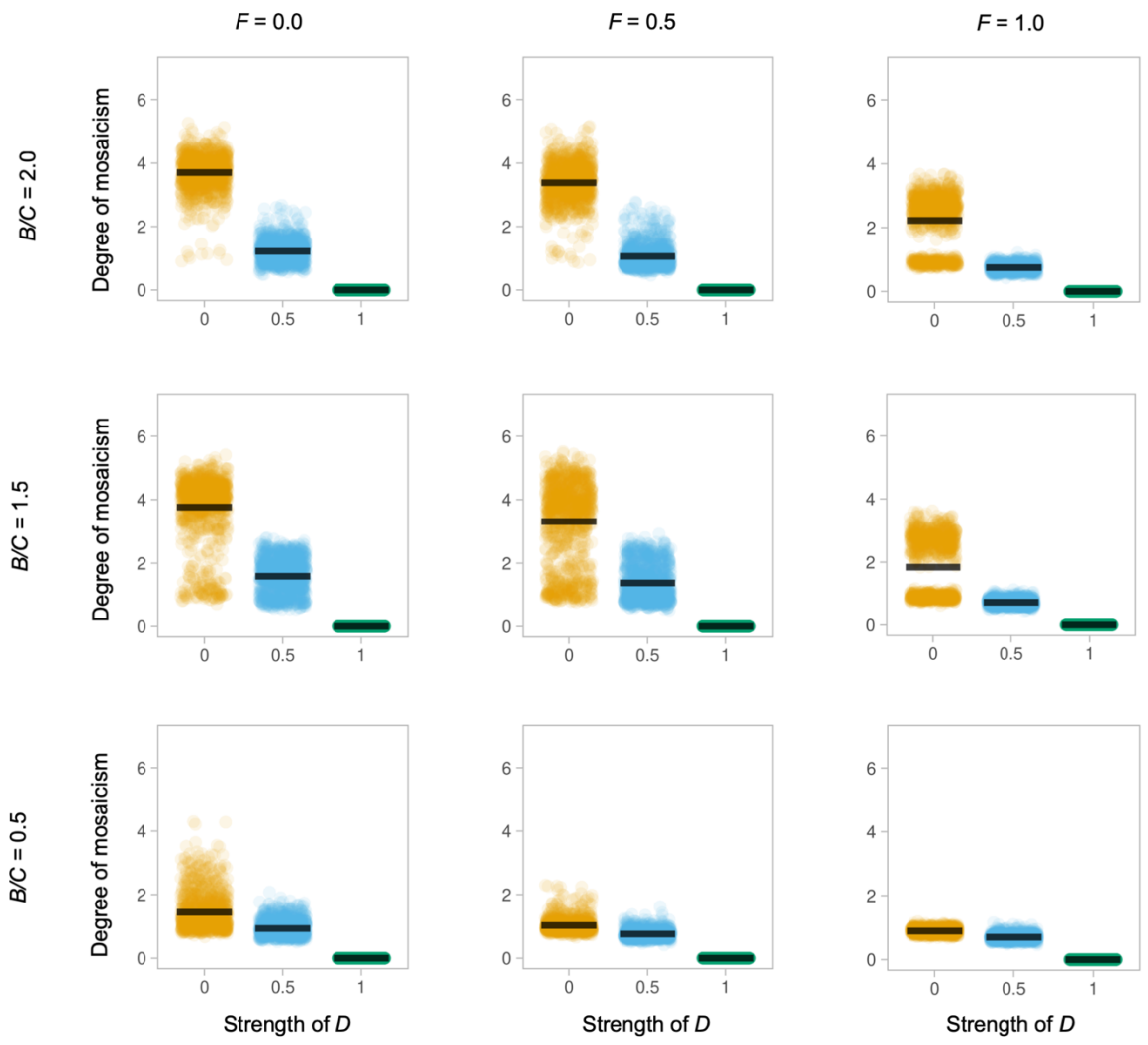

Figure S4: Evolution of 'mosaicism' under alternative conditions, with a mutation step size of 50%. Each plot depicts the 'degree of mosaicism' (y-axis, defined as the natural log of the ratio between the largest brain component and the smallest brain component in each individual, averaged across the population) as a function of developmental coupling *D* (x-axis) at the end of a 10-generation simulation run, compiled over 1,000 simulation runs, for a population of 100 individuals with an identical *D*, under different environments, defined by their functional coupling *F*, and their average benefit to cost ratio [extension of Figure 1].

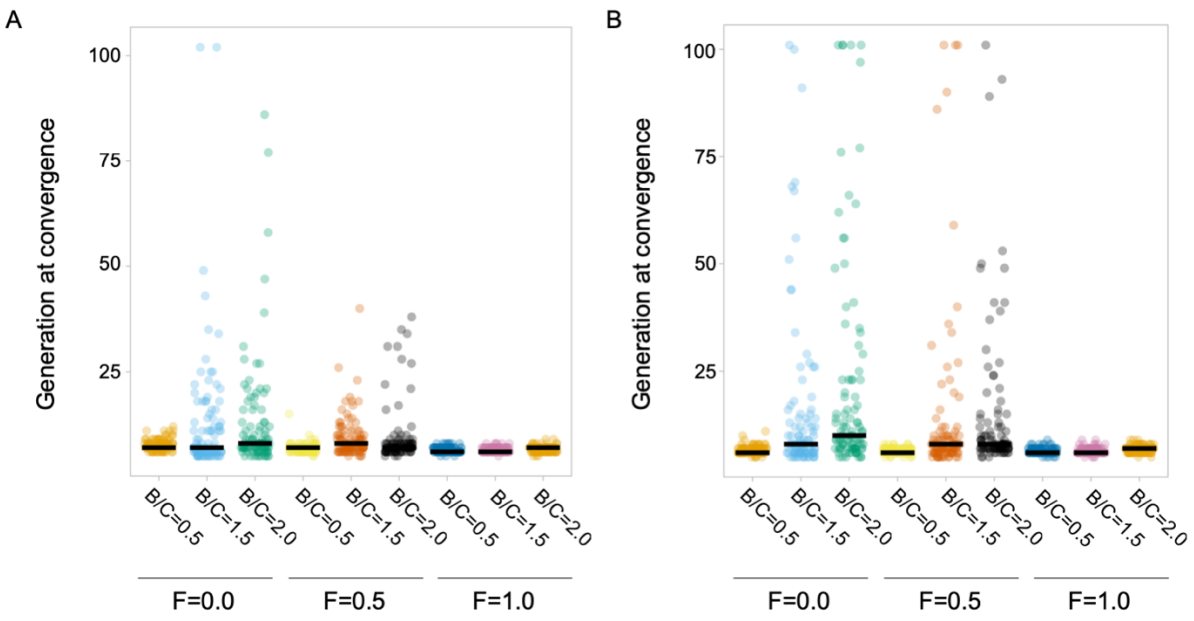

Figure S5: Generation number at convergence during simulations of competition between evolving populations with different *D*-strategies (*D* values) under alternative *F* and *B/C* conditions, and a 5% (A) or 50% (B) mutation step size. Convergence is defined as the generation at which one strategy represents 100% of individuals in the environment. Iterations at generation 150 had not yet converged on a single strategy. Convergence is slower when $F<1$ and $B>1$, where the difference in strategy success is less pronounced, and so multiple strategies persist for longer. Convergence is also slower with larger mutation sizes, as population means vary more between generations. [companion to Figure 2].

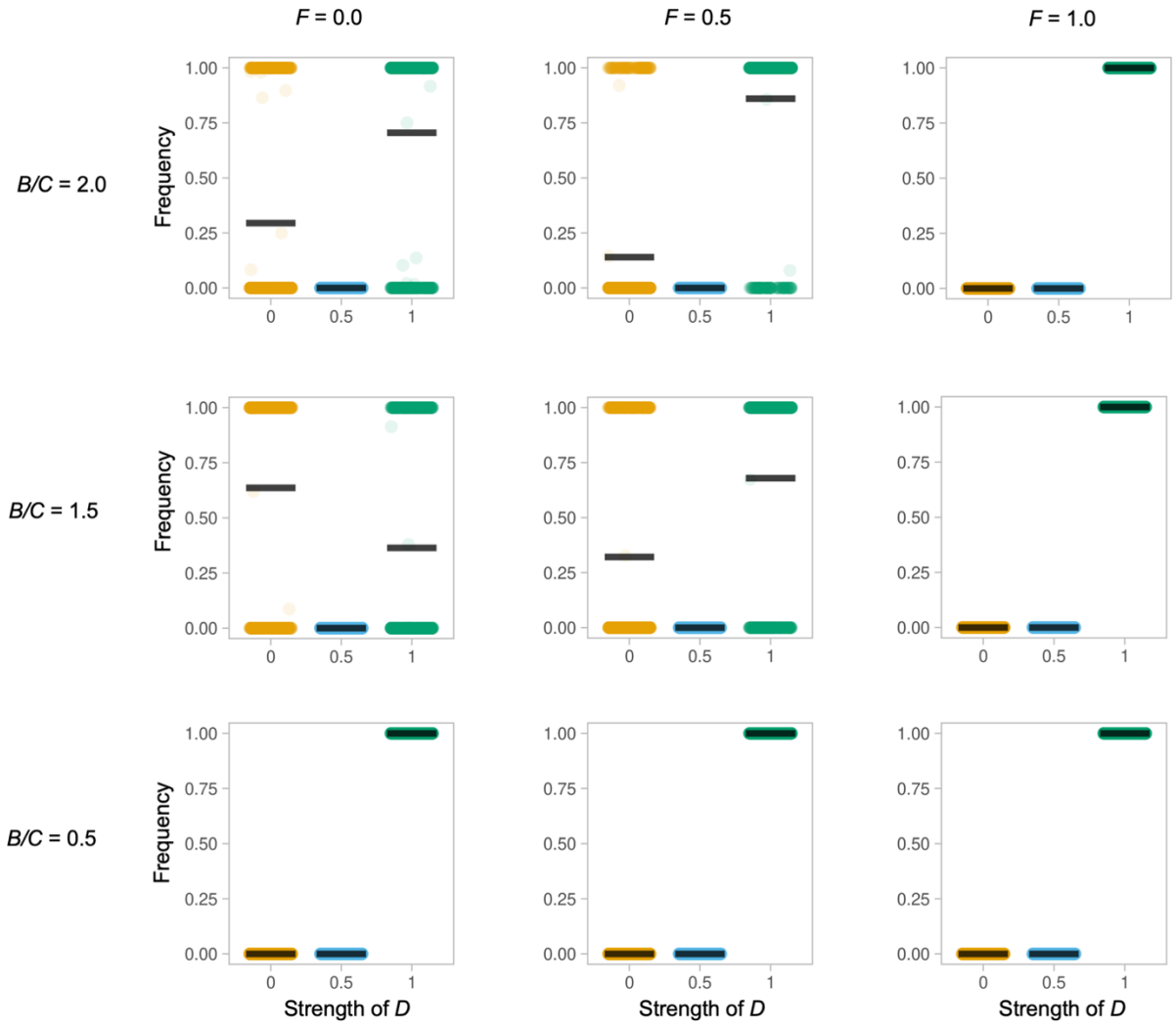

Figure S6: Competition between evolving populations with different *D*-strategies under alternative conditions, and a 5% mutation step size. Each plot depicts the ratio of that population to the total population (y-axis) as a function of developmental coupling *D* (x-axis) at the end of a 100-generation simulation run, compiled over 1,000 simulation runs, under alternative environments defined by their functional coupling *F,* and their average benefit to cost ratio. Populations are initialised such that there are 100 fully mosaic individuals (*D*=0.0), 100 hybrid individuals (*D*=0.5) and 100 concerted individuals (*D*=1.0). [sister to Figure 2].

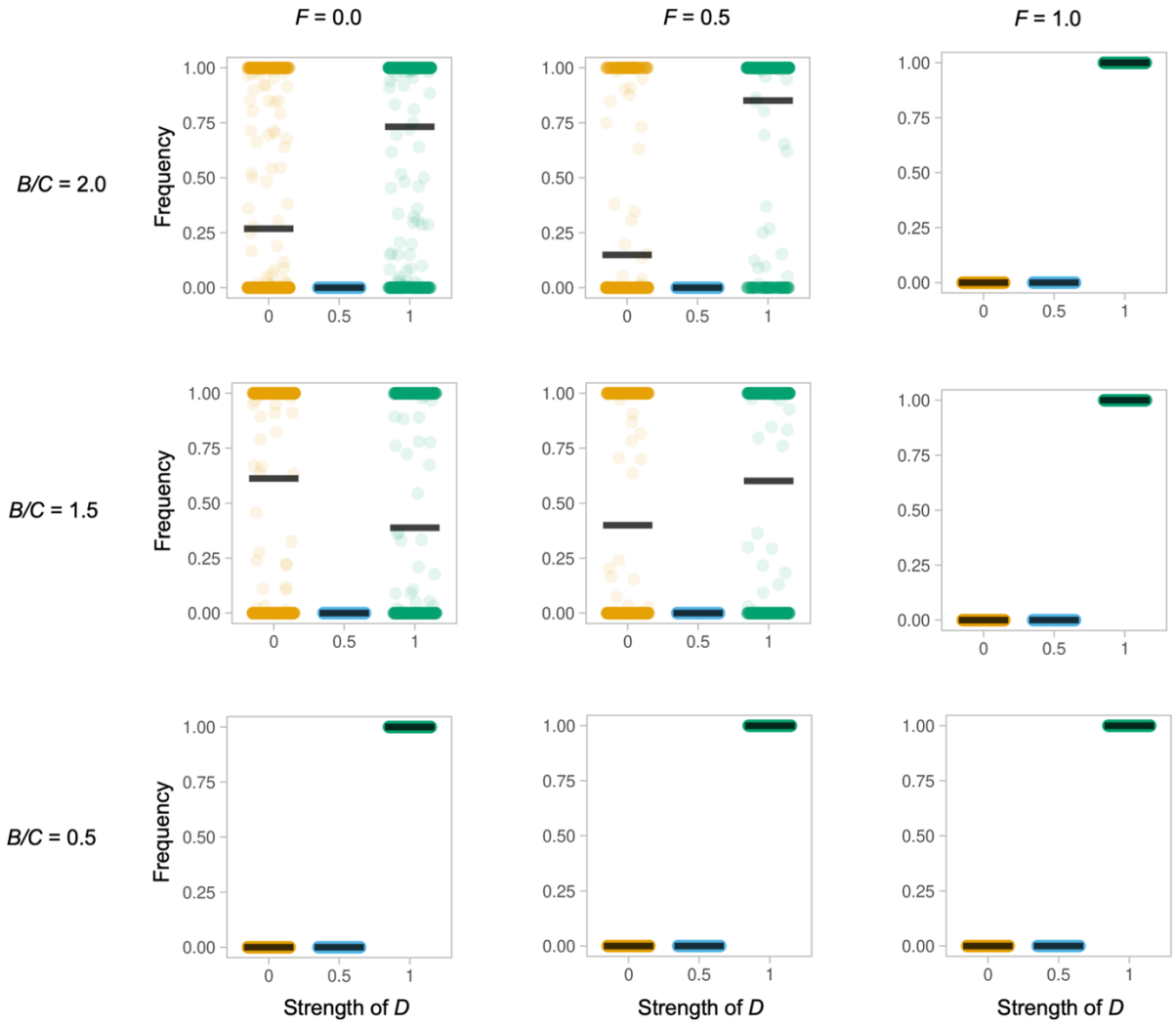

Figure S7: Competition between evolving populations with different *D*-strategies under alternative conditions, and a 50% mutation step size. Each plot depicts the ratio of that population to the total population (y-axis) as a function of developmental coupling *D* (x-axis) at the end of a 100-generation simulation run, compiled over 1,000 simulation runs, under alternative environments defined by their functional coupling *F,* and their average benefit to cost ratio. Populations are initialised such that there are 100 fully mosaic individuals (*D*=0.0), 100 hybrid individuals (*D*=0.5) and 100 concerted individuals (*D*=1.0) [extension of Figures 2 and 3].

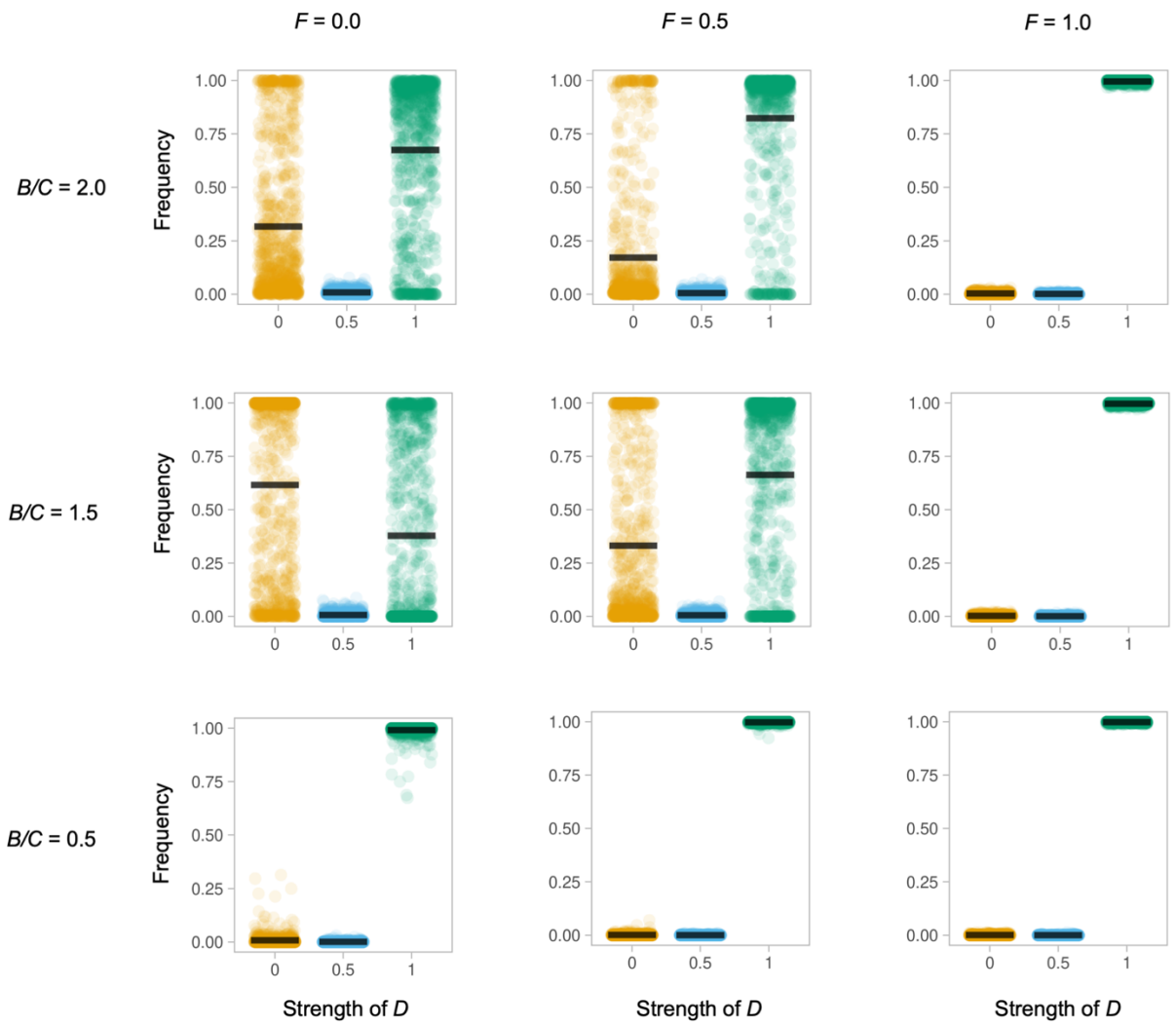

Figure S8: Competition between evolving populations with different *D*-strategies under alternative conditions, and a 50% mutation step size. Each plot depicts the ratio of that population to the total population (y-axis) as a function of developmental coupling *D* (x-axis) at the end of a 10-generation simulation run, compiled over 1,000 simulation runs, under alternative environments defined by their functional coupling *F,* and their average benefit to cost ratio. Populations are initialised such that there are 100 fully mosaic individuals (*D*=0.0), 100 hybrid individuals (*D*=0.5) and 100 concerted individuals (*D*=1.0) [extension of Figures 2 and 3].

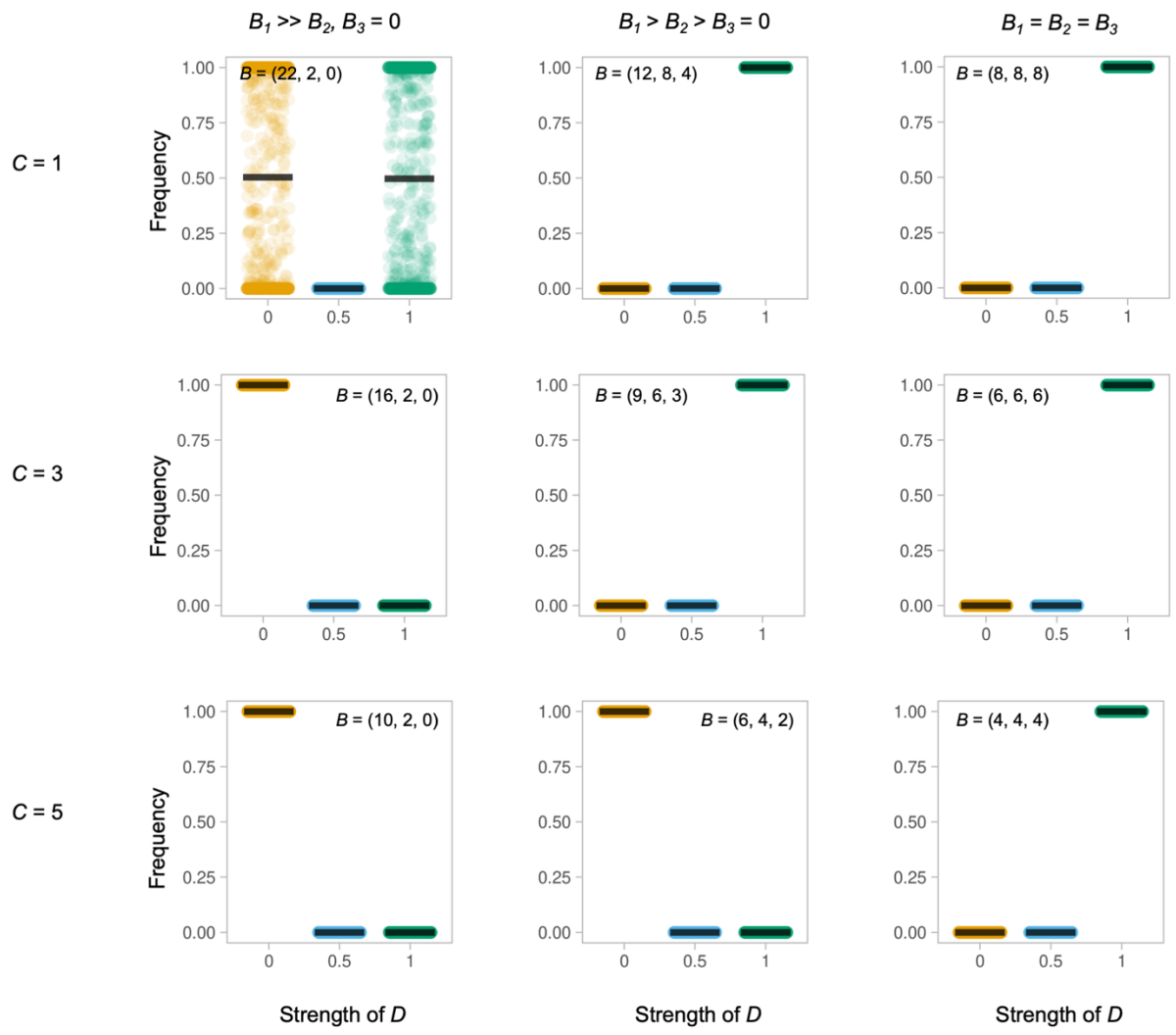

Figure S9: Competition between evolving populations with different *D*-strategies under alternative conditions, with a mutation step size of 5%. Each plot depicts the ratio of that population to the total population (y-axis) as a function of developmental coupling *D* (x-axis) at the end of a 100-generation simulation run, compiled over 1,000 simulation runs, with "hand-crafted" environments depicted in the table to explore specific situations of interest [extension of Figures 2 and 3].

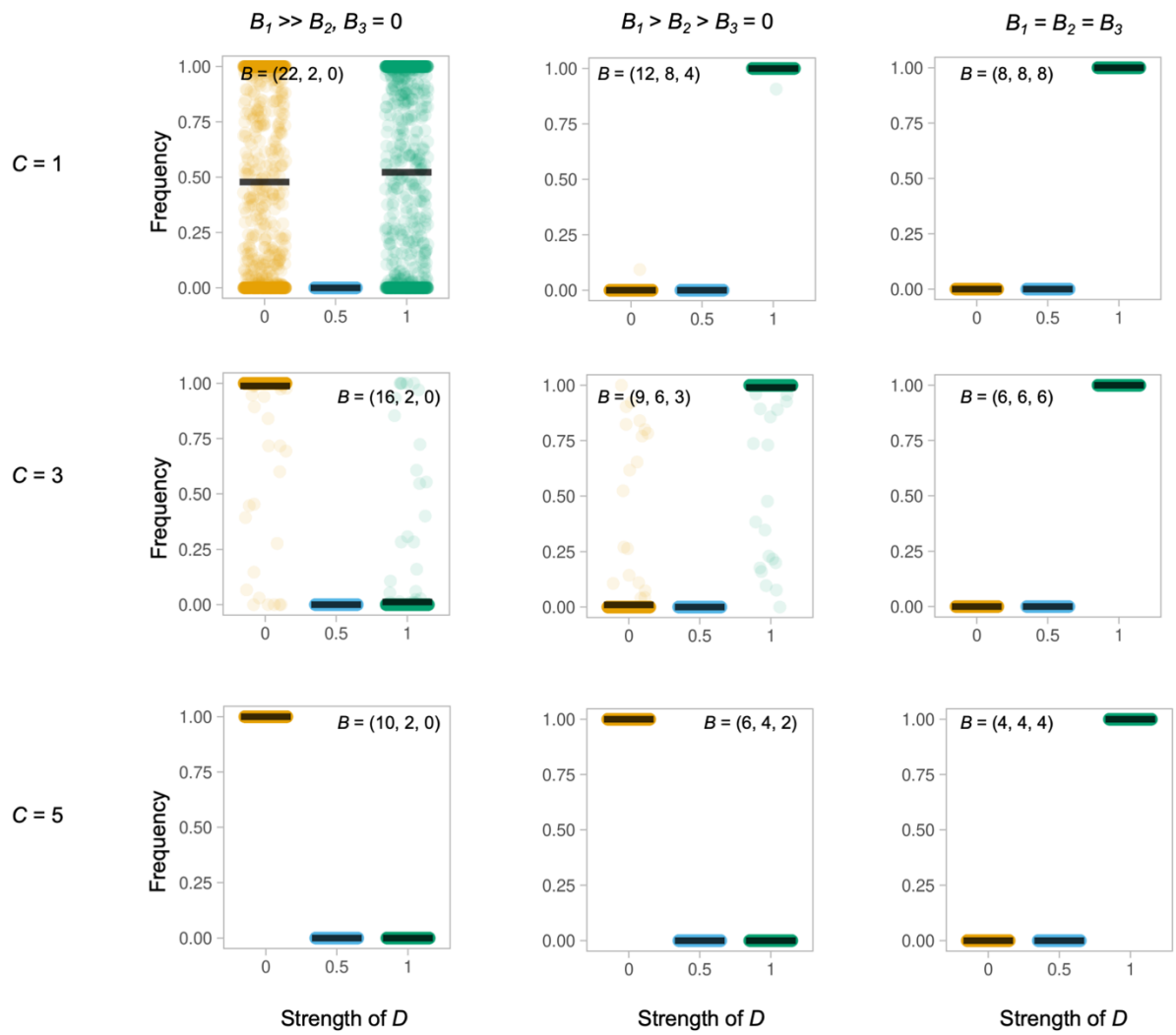

Figure S10: Competition between evolving populations with different *D*-strategies under alternative conditions, with a mutation step size of 50%. Each plot depicts the ratio of that population to the total population (y-axis) as a function of developmental coupling *D* (x-axis) at the end of a 100-generation simulation run, compiled over 1,000 simulation runs, with "hand-crafted" environments depicted in the table to explore specific situations of interest [extension of Figures 2 and 3].

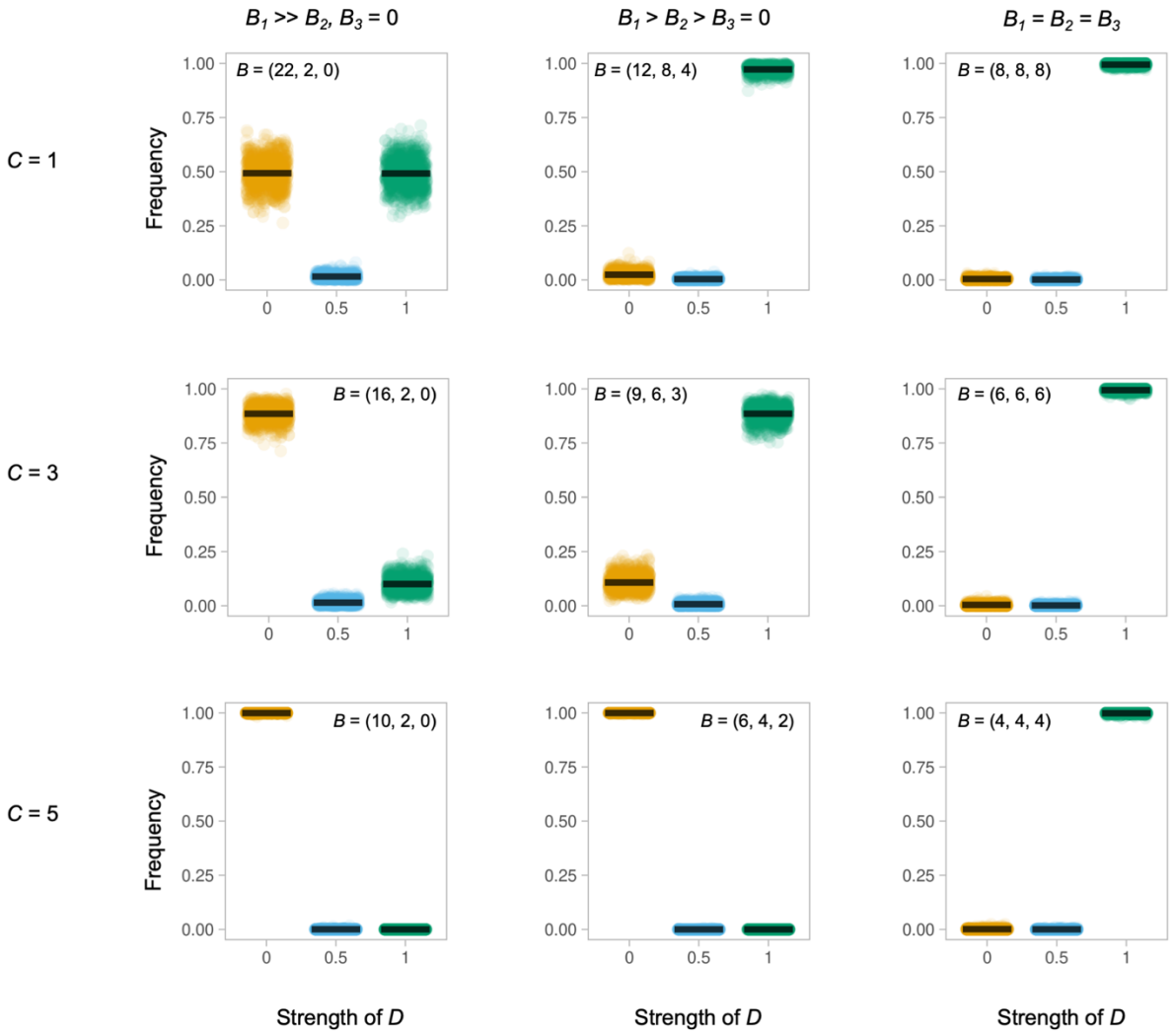

Figure S11: Competition between evolving populations with different *D*-strategies under alternative conditions, with a mutation step size of 50%. Each plot depicts the ratio of that population to the total population (y-axis) as a function of developmental coupling *D* (x-axis) at the end of a 10-generation simulation run, compiled over 1,000 simulation runs, with "hand-crafted" environments depicted in the table to explore specific situations of interest [extension of Figures 2 and 3].

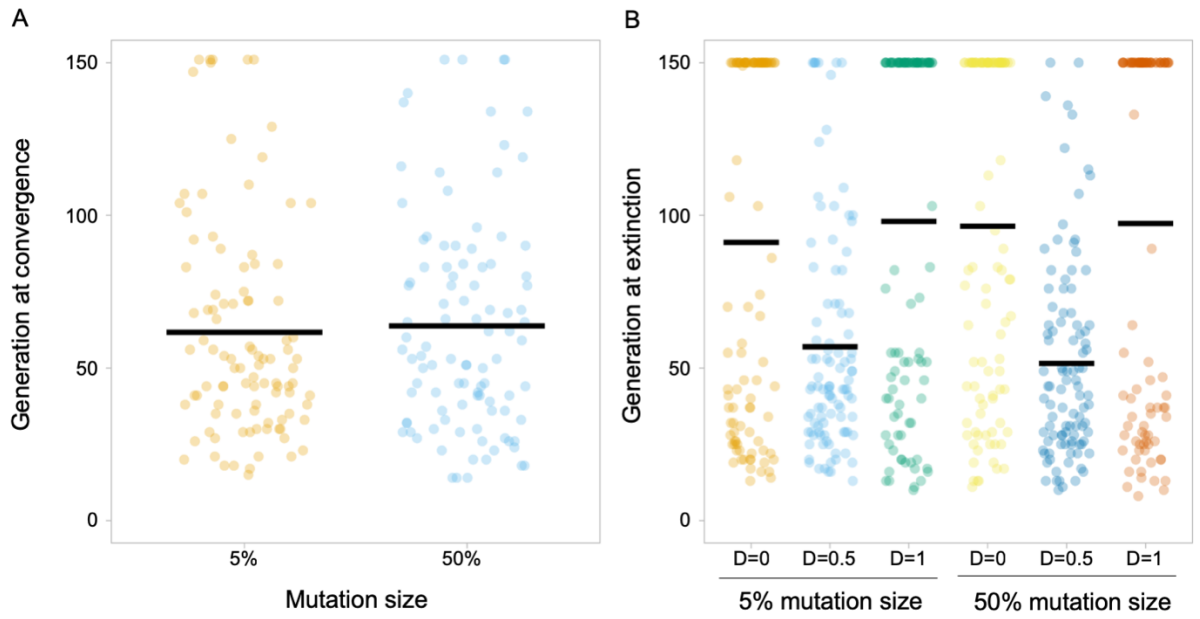

Figure S12: Conditions at convergence of simulations of competition between evolving populations with different *D*-strategies in a randomly varying environment, under different life history conditions. Convergence is defined as the generation at which one strategy represents 100% of individuals in the environment, extinction is defined as the generation at which a strategy drops to zero individuals. Iterations at generation 100 had not yet converged on a single strategy [companion to Figure 2].

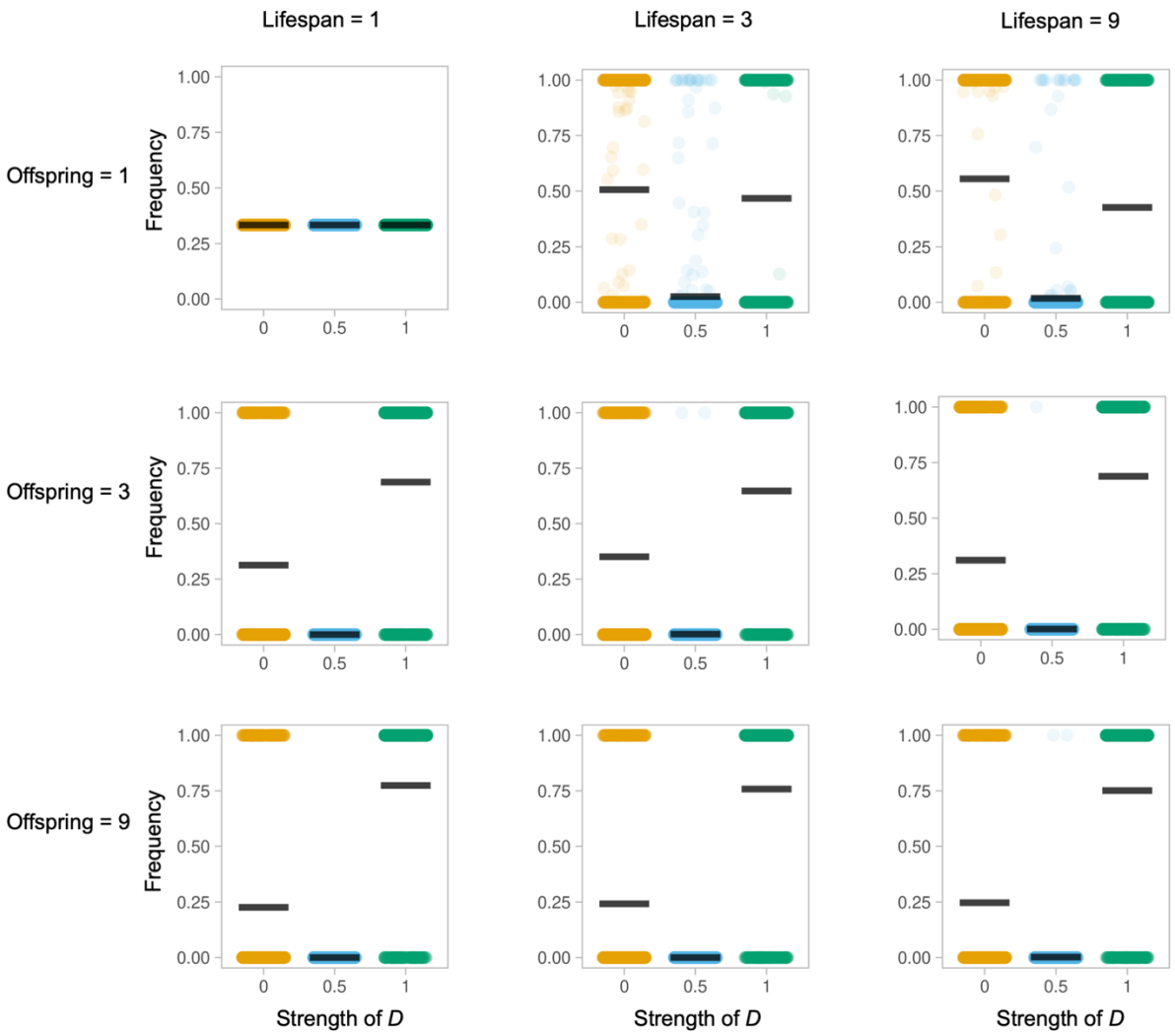

Figure S13: Competition between evolving populations with different *D*-strategies in a varying environment, under different life history conditions (lifespan, or number of generations an individual persists, and offspring number, which are generated every generation), with a 5% mutation step size. Each plot depicts the ratio of that population to the total population (y-axis) as a function of developmental coupling *D* (x-axis) at the end of a 150-generation simulation run, compiled over 1,000 simulation runs; every 2 generations the environment is replaced, using a uniform random distribution for cost [0.5, 5], max component benefit [1.0, 10], and *F* functional coupling [0, 1]. Populations are initialised such that there are 100 fully mosaic evolvers (*D*=0.0), 100 hybrid evolvers (*D*=0.5) and 100 concerted evolvers (*D*=1.0) [sister to Figure 4].

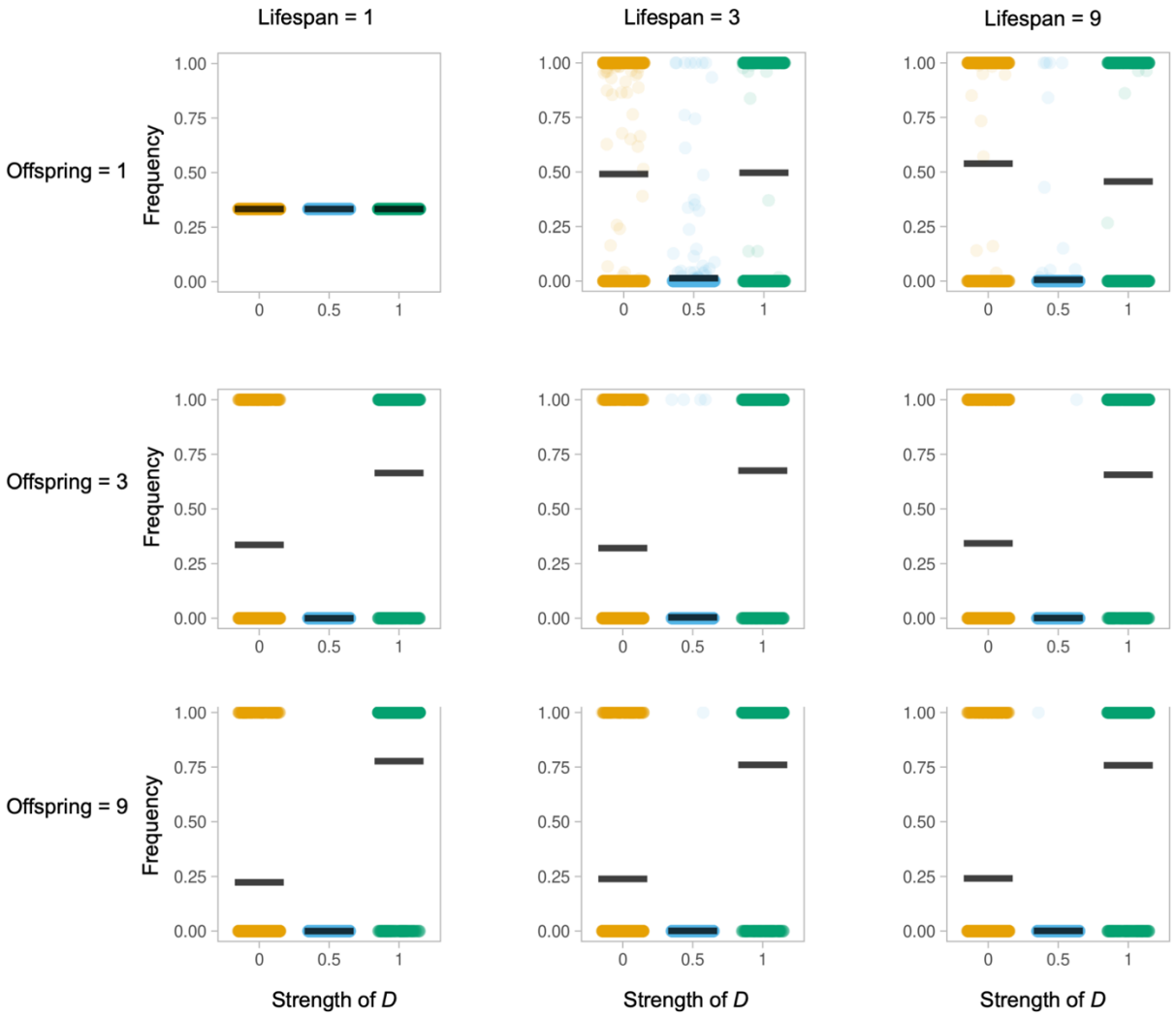

Figure S14: Competition between evolving populations with different *D*-strategies in a varying environment, under different life history conditions (lifespan, or number of generations an individual persists, and offspring number, which are generated every generation), with a 50% mutation step size. Each plot depicts the ratio of that population to the total population (y-axis) as a function of developmental coupling *D* (x-axis) at the end of a 150-generation simulation run, compiled over 1,000 simulation runs; every 2 generations the environment is replaced, using a uniform random distribution for cost [0.5, 5], max component benefit [1.0, 10], and *F* functional coupling [0, 1]. Populations are initialised such that there are 100 fully mosaic evolvers (*D*=0.0), 100 hybrid evolvers (*D*=0.5) and 100 concerted evolvers (*D*=1.0) [sister to Figure 4].

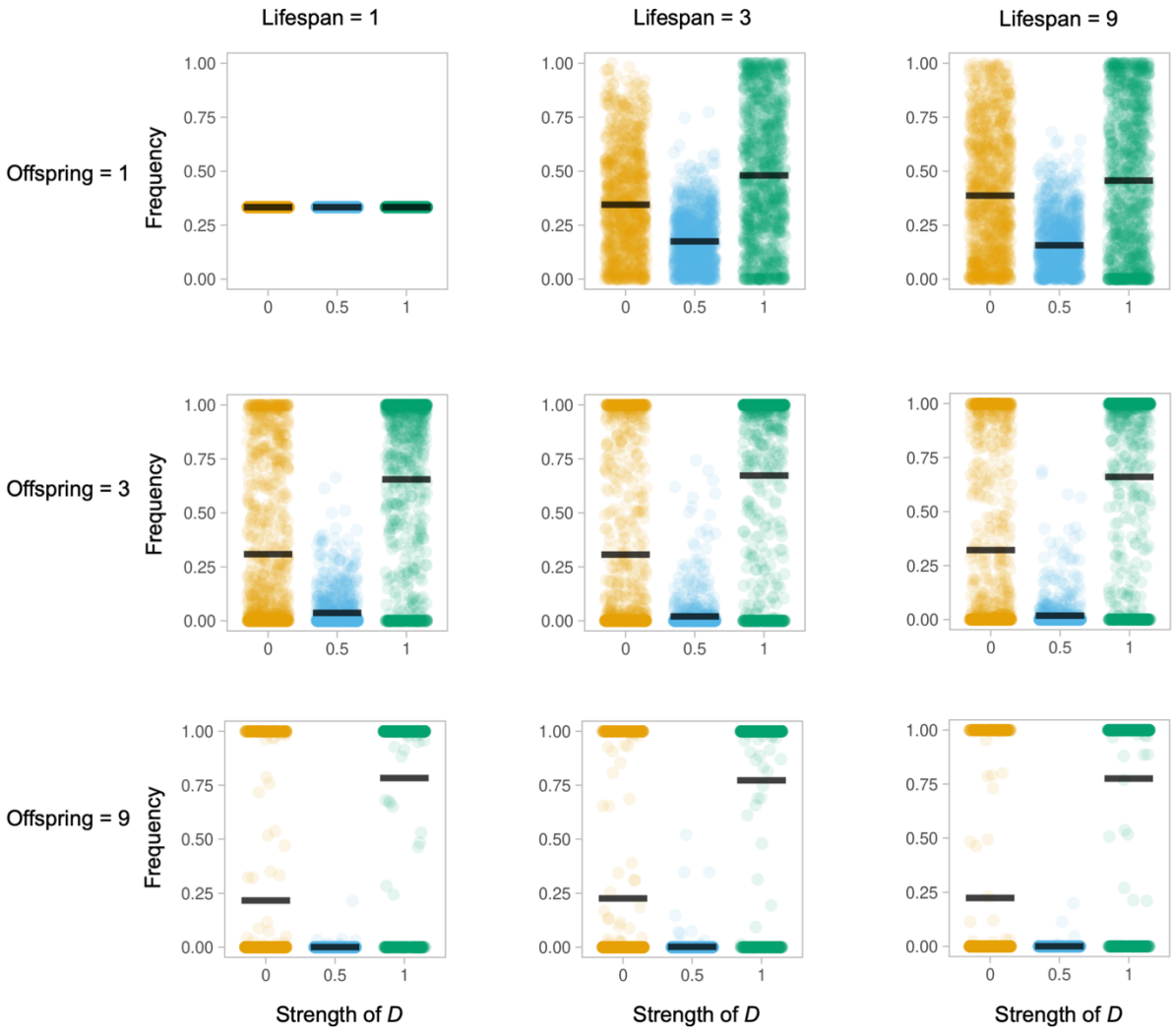

Figure S15: Competition between evolving populations with different *D*-strategies in a varying environment, under different life history conditions (lifespan, or number of generations an individual persists, and offspring number, which are generated every generation), with a 5% mutation step size. Each plot depicts the ratio of that population to the total population (y-axis) as a function of developmental coupling *D* (x-axis) at the end of a 10-generation simulation run, compiled over 1,000 simulation runs; every 2 generations the environment is replaced, using a uniform random distribution for cost [0.5, 5], max component benefit [1.0, 10], and *F* functional coupling [0, 1]. Populations are initialised such that there are 100 fully mosaic evolvers (*D*=0.0), 100 hybrid evolvers (*D*=0.5) and 100 concerted evolvers (*D*=1.0) [sister to Figure 4].

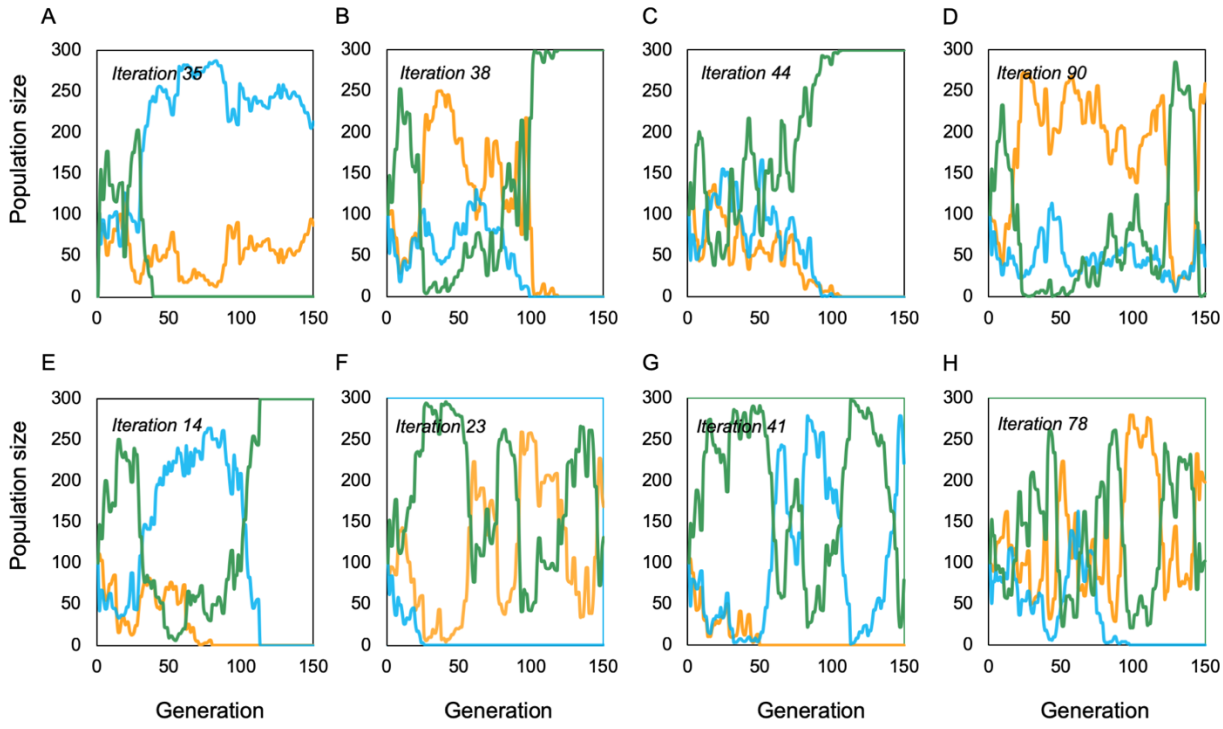

Figure S16: Selected, representative, individual simulations showing fluctuations in population frequencies over generations for a 5% mutation size (A-D) or a 50% mutation size (E-H). Colours indicate the *D*-strategies, or *D* value, where yellow is *D* =0, where blue is *D* =0.5, and where green is *D* =1. These examples illustrate the central conclusion from this set of simulations, that multiple strategies can persist across time together. We interpret this as suggesting allelic variation for concerted and mosaic evolution could be maintained in a population under fluctuating environmental conditions, and hence be available to selection. [extension of Figure 4].

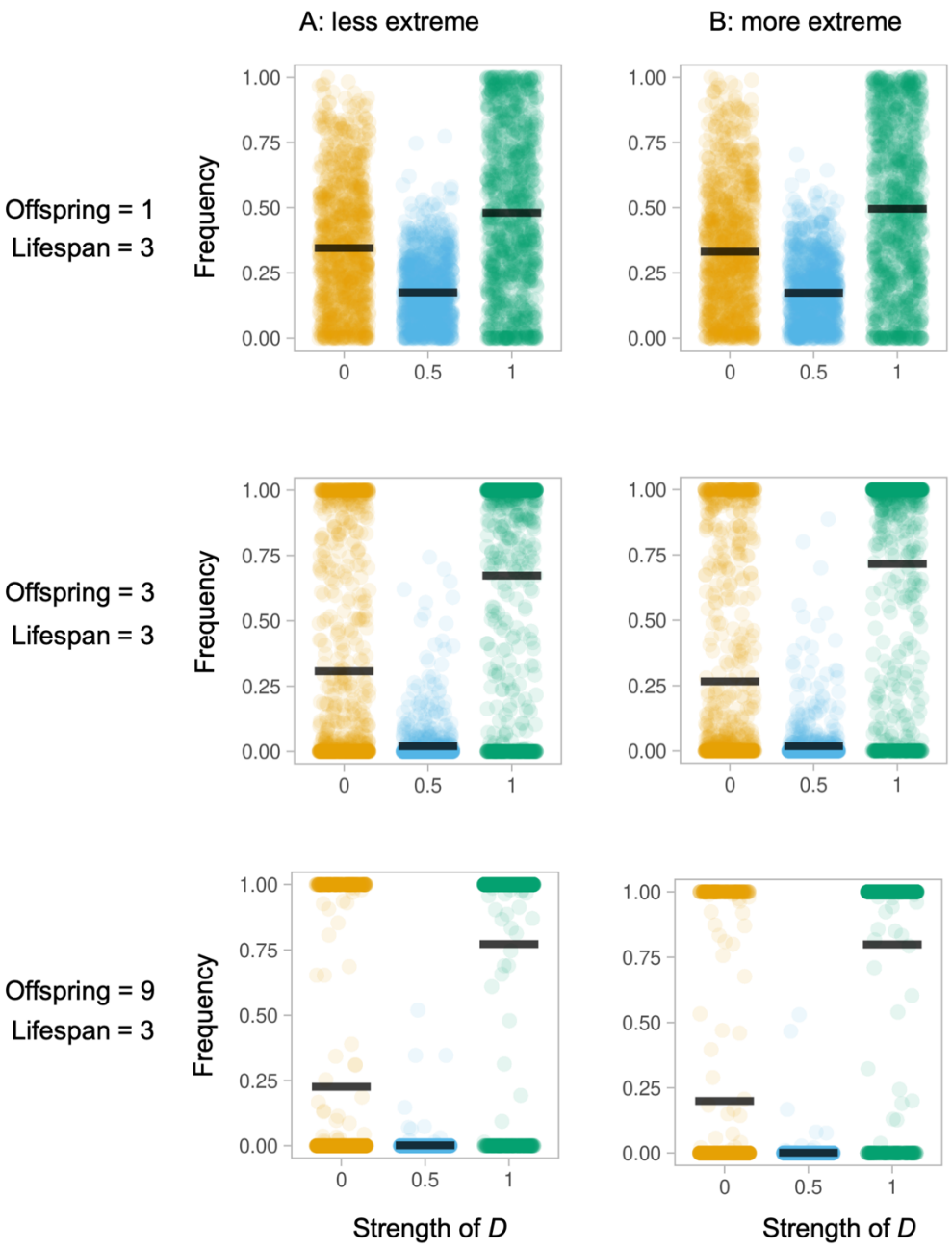

Figure S17: Competition between evolving populations with different *D*-strategies in a varying environment, under selected life history conditions, as described for Figure S15 (column A), but with an increased distribution for cost [0, 10] and max average benefit [0, 30] creating more 'extreme' environmental fluctuations (column B). During early generations of the simulations, more extreme environmental fluctuations increase the probability of a concerted strategy being successful, as indicated by a significant interaction between *D* and the size fluctuation size category ($t = 8.986$, $p<0.001$), but with a low effect size. [extension of Figure S16].

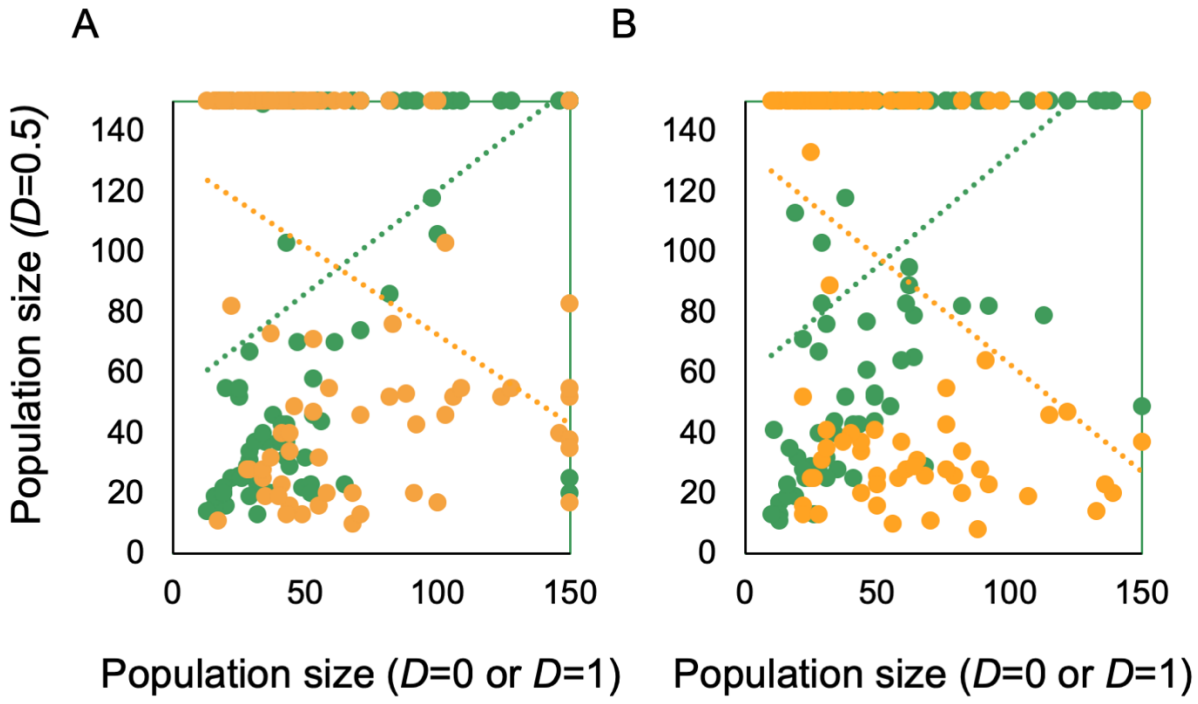

Figure S18: Relationship between population frequencies between partially mosaic brains (*D*=0.5) and fully mosaic (*D*=0), or concerted brains (*D*=1) from simulations in varying environmental conditions and a 5% mutation size (A) or 50% mutation size (B). The plot shows that *D*=0 and *D*=0.5 are more commonly favoured in the same environments (shown in green) than *D*=0 and *D*=1.0 (shown in yellow) [extension of Figure 4].